Review

A Review of Irrigation Information Retrievals from Space and Their Utility for Users

Christian Massari [1,*], Sara Modanesi [1,2,3], Jacopo Dari [1,4], Alexander Gruber [2], Gabrielle J. M. De Lannoy [2], Manuela Girotto [5], Pere Quintana-Seguí [6], Michel Le Page [7], Lionel Jarlan [7], Mehrez Zribi [7], Nadia Ouaadi [7,8], Mariëtte Vreugdenhil [9], Luca Zappa [9], Wouter Dorigo [9], Wolfgang Wagner [9], Joost Brombacher [10], Henk Pelgrum [10], Pauline Jaquot [10], Vahid Freeman [11], Espen Volden [12], Diego Fernandez Prieto [12], Angelica Tarpanelli [1], Silvia Barbetta [1] and Luca Brocca [1]

1   Research Institute for the Geo-Hydrological Protection, National Research Council (CNR), Via Madonna Alta 126, 06128 Perugia, Italy; sara.modanesi@irpi.cnr.it (S.M.); jacopo.dari@unipg.it (J.D.); angelica.tarpanelli@irpi.cnr.it (A.T.); silvia.barbetta@irpi.cnr.it (S.B.); luca.brocca@irpi.cnr.it (L.B.)
2   Department of Earth and Environmental Sciences, KU Leuven, Celestijnenlaan 200e, 3001 Leuven, Belgium; alexander.gruber@kuleuven.be (A.G.); gabrielle.delannoy@kuleuven.be (G.J.M.D.L.)
3   Department of Civil and Environmental Engineering (DICEA), University of Florence, Via di S. Marta 3, 50139 Firenze, Italy
4   Department of Civil and Environmental Engineering, University of Perugia, Via G. Duranti 93, 06125 Perugia, Italy
5   Department of Environmental Science and Policy Management, University of California, 130 Mulford Hall #3114 Berkeley, Berkeley, CA 94720-3114, USA; mgirotto@berkeley.edu
6   Observatori de l'Ebre, Universitat Ramon Llull, Carrer Horta Alta 38, 43520 Roquetes, Spain; pquintana@obsebre.es
7   CESBIO, CNES/CNRS/INRAE/IRD/UPS, 18 Avenue Edouard Belin, Université de Toulouse, CEDEX 9, 31401 Toulouse, France; michel.le_page@ird.fr (M.L.P.); lionel.jarlan@ird.fr (L.J.); mehrez.zribi@ird.fr (M.Z.); nadia.ouaadi@univ-tlse3.fr (N.O.)
8   LMFE, Department of Physics, Faculty of Sciences Semlalia, Cadi Ayyad University, Marrakech 4000, Morocco
9   Department of Geodesy and Geoinformation, Technische Universität Wien (TU Wien), Wiedner Hauptstraße 8-10, 1040 Vienna, Austria; mariette.vreugdenhil@geo.tuwien.ac.at (M.V.); luca.zappa@geo.tuwien.ac.at (L.Z.); wouter.dorigo@geo.tuwien.ac.at (W.D.); wolfgang.wagner@geo.tuwien.ac.at (W.W.)
10   eLEAF Competence Center, Research & Development, Hesselink van Suchtelenweg 6, 6703CT Wageningen, The Netherlands; joost.brombacher@eleaf.com (J.B.); henk.pelgrum@eleaf.com (H.P.); pauline.jaquot@eleaf.com (P.J.)
11   Spire Global, 33 Rue Sainte Zithe, 2763 Luxembourg, Luxembourg; vahid.freeman@spire.com
12   European Space Agency (ESA), Via Galileo Galilei, 1, Frascati, 00044 Roma, Italy; Espen.Volden@esa.int (E.V.); Diego.Fernandez@esa.int (D.F.P.)
*   Correspondence: christian.massari@irpi.cnr.it

Abstract: Irrigation represents one of the most impactful human interventions in the terrestrial water cycle. Knowing the distribution and extent of irrigated areas as well as the amount of water used for irrigation plays a central role in modeling irrigation water requirements and quantifying the impact of irrigation on regional climate, river discharge, and groundwater depletion. Obtaining high-quality global information about irrigation is challenging, especially in terms of quantification of the water actually used for irrigation. Here, we review existing Earth observation datasets, models, and algorithms used for irrigation mapping and quantification from the field to the global scale. The current observation capacities are confronted with the results of a survey on user requirements on satellite-observed irrigation for agricultural water resources' management. Based on this information, we identify current shortcomings of irrigation monitoring capabilities from space and phrase guidelines for potential future satellite missions and observation strategies.

Keywords: irrigation; satellite; soil moisture; evapotranspiration; water cycle; farmers

check for updates

1. Introduction

Irrigated agriculture accounts for more than 70 percent of the water withdrawn worldwide from lakes, rivers, and aquifers [1], in many countries even for more than 90 percent, thus being the greatest human disturbance in the terrestrial water cycle [2]. Even though only 17 percent of global crop land is irrigated, these lands already produce 40 percent of the world's food [3]. Since the global demand for food will further increase in the next decades due to population growth and dietary shifts, keeping pace with this growing demand will require even further expansion and intensification of irrigated agriculture [4,5].

At the same time, urbanization pressure, market volatility, and climate variability associated with an increased recurrence and intensity of drought periods [6–8] have led to a call for improved water management involving reducing water withdrawals and increasing irrigation efficiency.

Meeting these ends will require: (1) modeling irrigation water requirements at the global scale [9], (2) assessing irrigated food production [10], (3) quantifying the impact of irrigation on climate [11], river discharge [12], and groundwater depletion [13,14], and (4) building plans for an optimal water resource allocation so that managers can accurately account for water use [15–17]. Central to all these steps is accurate knowledge about the spatial extent of irrigated lands, the amount of water applied as irrigation, and the timing when irrigation is applied.

Obtaining this information with a high quality and on a global scale, however, is not trivial. Many wells are located on private lands, are used for small-scale agriculture, and are often illegal due to the reluctance of farmers to drill wells with official permission to avoid regulations [18].

Consequently, the overwhelming majority of agricultural water use worldwide—both from groundwater and surface water—remains unmetered [19].

Earth observing satellites provide the unique ability to monitor various processes strongly related to irrigation, e.g., soil moisture, land cover, or vegetation activity, quasi-globally and frequently. In the last decade, there has been a significant interest in using satellite Earth observations to retrieve information on irrigation extent, frequency, and amount. This has led to a proliferation of studies using new satellite platforms able to measure surface variables with relatively high spatial resolutions (i.e., less than 1 km) [20]. Many studies have also attempted to include irrigation modules in land surface models or ingest satellite observations to correct for the lack of irrigation representation.

The main objectives of this study are:

- To provide a comprehensive review of studies that have attempted to map irrigation, more specifically (i) where irrigation occurs, i.e., mapping methods, (ii) when irrigation occurs (frequency of irrigation), i.e., timing methods, and (iii) how much irrigation is applied. Reviewed studies include: (i) methods based on ground measurements and local statistics, (ii) remote sensing-based methods including multispectral, microwave, and gravimetric measurements, and (iii) methods based on modeling and data assimilation.
- To report the results of a survey about user requirements on irrigation management in small-scale farming that targeted ten companies and organizations representative of the Mediterranean area (Spain, Italy, and France).
- To confront the review of irrigation mapping studies with the user requirements survey in order to assess whether current remote sensing and modeling-based irrigation products can meet the requirements of actors working in the field of water resource management and agriculture.
- To provide recommendations and guidelines for the future development of improved irrigation mapping techniques to help us meet the demands of farmers and stakeholders.

The manuscript is organized as follows: Section 2 lists previous efforts to map irrigation using national statistics and ground observations. Section 3 presents methods and techniques used to retrieve irrigation information from Earth observation. Section 4

reviews irrigation mapping studies that are based on modeling and data assimilation. Section 5 discusses user needs and the degree to which current irrigation information retrieved from satellites (and models) meet them. Section 6 provides a synthesis of the review results and future perspectives and can guide the reader to disentangle among the huge number of studies in the field by listing the main results and conclusions (the reader interested in a general overview of the topic can skip directly to this section).

2. Irrigation Mapping with Ground Observations and National Statistics

The first digital global map of Irrigated Areas (GMIA, [9]) was produced at a resolution of 0.5° (see Figure 1a as an example for India). The map was mainly based on a compilation of outlines of main irrigation areas and the FAO total area in a country between 1990 and 1995 and is based on an inventory of subnational irrigation statistics.
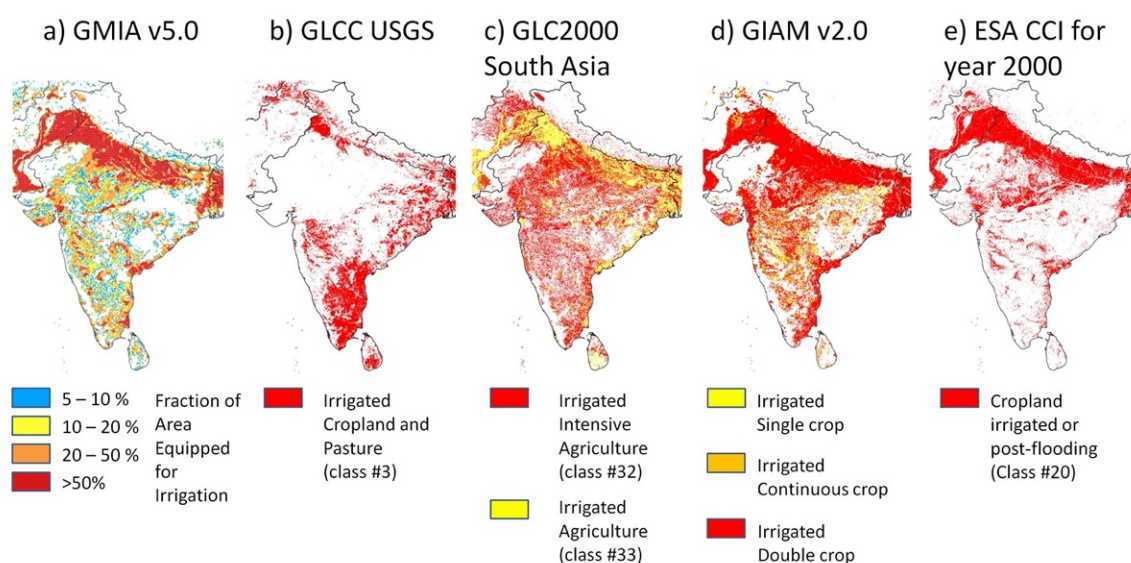

Figure 1. Mapping of irrigation in India according to (**a**) GMIA 5.0 [9], (**b**) Global Land Cover Characteristic (GLCC) USGS Land Use/Land Cover System [21], (**c**) GLC2000 for South Asia [22], (**d**) GIAM v2.0 [23], and (**e**) ESA CCI for the year 2000 [24].

This dataset was also the base for a derived dataset including crop calendars of irrigated crops [25]. Later, Siebert et al. [26,27] developed the global Historical Irrigation dataset (HID) by collecting subnational irrigation statistics from various sources to estimate the temporal development of irrigated areas between 1900 and 2005 at a resolution of 5 arcmin.

All of these maps provide the so-called "Area Equipped for Irrigation (AEI)", as defined by FAO, which was inventoried by national or local authorities (Figure 1 shows an example of the AEI of the different datasets plotted over India). However, despite being very important, AEI are based upon agricultural statistics which may be outdated or inaccurate [26]. For example, the abandonment of irrigation infrastructures in former soviet countries is not accounted for, while the expansion of irrigated areas based on groundwater is often not included in the AEI. Despite these limitations, this dataset remains a reference for many potential applications, including global hydrological modeling, the modeling of changes in crop productivity, or climate impact assessments.

3. Irrigation Remote Sensing

Since the 1970s, studies have started using remotely sensed images from Landsat-1 to map irrigated areas and estimate water use [28]. While first images were analyzed visually, research has advanced rapidly in the last decades, where now a multitude of methods are available.

We reviewed the status of research in methods for retrieving irrigation information from space by systematically reviewing relevant literature in the topic resulting from the most important databases, such as Scopus, Web of Science, and Google Scholar. Only papers after 2000 were taken into consideration and we selected those (i) introducing innovative techniques to retrieve irrigation information, and (ii) using new type of Earth observation in relation to the publication period. More than 50 manuscripts were reviewed, from which we extracted details on the type of information retrieved (i.e., mapping or quantification), study area, method and type of Earth observation used, spatial scale at which this information was provided, and, when available, the associated accuracy (see Table 1 for a summary of the results). Below, we provide a synthesis of the methodological approaches reviewed, organized based on the main Earth observation technique.

Table 1. Summary of relevant literature on the irrigation detection and quantification using satellite amount. Key results indicate the ability of the technique to map ("mapping", i.e., detect irrigated areas) and quantify applied irrigation volumes ("quantification"). The technique column indicates the main method used among visible- and near-infrared sensors (VIS/NIR), Microwave (MW), Land Surface models (LSM), and Energy balance models (EBM).

Technique	Spatial Scale/Sampling (Sensor Used)	Key Results	Reference
VIS/NIR	30 m Landsat	Mapping	Thenkabail et al. (2006), Peña-Arancibia et al. (2014), Deines et al. (2017), Deines et al. (2019)
	250 m, 500 m MODIS, MERIS	Mapping	Ambika et al. (2016), Ozdogan and Gutman (2008), Pervez et al. (2010), Salmon et al. (2015)
	~1 km AVHHR	Mapping	Thenkabail et al. (2006)
	30 m HJ-1A/B	Mapping	Jin et al. (2016)
	30 m MODIS + Landsat OLI	Mapping	Chen et al. (2018)
	500 m MODIS	Quantification	Vogels et al. (2020)
	20 m—plot scale Sentinel 2	Quantification	Maselli et al. (2020)
Mix of VIS/NIR, MW, LSM and EBM	~30 min Meteosat-9 ET + Water balance	Quantification	Romaguera et al. (2014)
	Basin-scale MODIS plus WEAP and MODFLOW models	Quantification	Le Page et al. (2012)
	~25 km ERA5 + MODIS	Mapping	Zohaib et al. (2019)
	30 m SEBS + Landsat	Mapping	Pun et al. (2017)
	30 m Landsat data + SWAP	Quantification	Droogers et al. (2010), Olivera-Guerra et al. 2020
	500m Noah-MP + MODIS	Mapping and quantification	Ozdogan et al. (2010)
	Basin-wide results MODIS, MeteoSat Second Generation (MSG), SEBAL	Quantification	Van Eekelen et al. (2015)

Table 1. *Cont.*

Technique	Spatial Scale/Sampling (Sensor Used)	Key Results	Reference
	0.05° ALEXI based on GOES satellite + Noah LSM	Quantification	Yilmaz et al. (2014)
	~4 km ALEXI based on GOES satellite + Noah LSM	Quantification	Hain et al. (2015)
	MODIS ET + Hydrological model Basin scale	Quantification	Peña-Arancibia et al.
	3 m CubSats + PT-JPL model	Quantification	Aragon et al. (2018)
	1 km ET-Look	Quantification	Bastiaanssen et al. (2014)
MW+LSM	~25–50 km AMSR-E, AMSR2, ASCAT, SMOS, WindSat + Noah LSM	Mapping	Kumar at al. (2015)
	1/5/25 km AMSR2, ASCAT, SMOS + SURFEX LSM	Mapping	Escorihuela and Quintana-Seguí (2016)
	25 km AMSR2, ASCAT, SMAP + MERRA-2 reanalysis	Quantification	Zaussinger et al. (2019)
	1/9/12.5 km ASCAT, Sentinel-1, SMAP, SMOS + SURFEX LSM	Mapping	Dari et al. (2021)
Gravimetric measurements + LSM	0.125° Noah-MP +GRACE	Quantification	Nie et al. (2019)
	36 km CLSM + GRACE	Quantification	Girotto et al. (2017)
MW + VIS/NIR	1–25 km AMSR-E + SPOT-VEG	Mapping	Singh et al. (2017)
	10–20 m Sentinel 1 + Sentinel 2	Mapping	Ferrant et al. (2017), Ferrant et al. (2019), Pageot et al. (2020), Le Page et al. (2020)
	Plot-scale Sentinel 1 + Sentinel 2	Mapping	Bousbih et al. (2018)
	Plot-scale Sentinel 1 + Sentinel 2	Mapping	Bazzi et al. (2019)
	Plot-scale Sentinel 1 + Sentinel 2	Mapping	Bazzi et al. (2020)
	30 m Sentinel 1 + Landsat	Mapping	Demarez et al. (2019)
MW	3 m TSK 8 m CSK	Mapping	El Hajj et al. (2014)
	9 km SMAP	Mapping	Lawston et al. (2017)
	Plot-scale Sentinel 1	Mapping	Gao et al. (2018)
	25 km AMSR2, ASCAT, SMAP, SMOS	Quantification	Brocca et al. (2018)

Table 1. *Cont.*

Technique	Spatial Scale/Sampling (Sensor Used)	Key Results	Reference
	25 km AMSR2	Quantification	Jalilvand et al. (2019)
	1 km SMOS	Mapping	Malbéteau et al. (2018)
	0.25° AMSR-E, AMSR2, ASCAT, ESA CCI	Mapping	Zhang et al. (2018)
	1 km SMAP, SMOS	Quantification	Dari et al. (2020)
	500 m Sentinel 1	Quantification	Zappa et al. (2021)

3.1. Visible- and Near-Infrared-Based Methods

Visible- and near-infrared measurements can be used (i) to detect changes in vegetation greenness, health, and water content represented by empirical vegetation indices, (ii) to retrieve land surface temperature, and (iii) to model evapotranspiration. All these types of information potentially facilitate irrigation mapping and monitoring and indeed, many different strategies have been developed to do so, as will be described in the following sections.

3.1.1. Mapping Methods

Data from optical sensors including Landsat, MODIS (Moderate Resolution Imaging Spectroradiometer), AVHRR (Advanced Very High-Resolution Radiometer), MERIS (Medium, Resolution Imaging spectrometer), and SPOT (Satellite pour l'Observation de la Terre) [4,29–32], and their combination with other model-based and ground-based ancillary data [33], have been extensively used to map irrigated areas, making use of the difference in the spectral responses of irrigated and non-irrigated croplands. One of the first explicit attempts to use visible- and near-infrared remote sensing information for the detection of irrigated areas at the global scale is the International Water Management Institute Global Irrigated Area Map [23]. This dataset represented the irrigated areas of the world in 1999 with a resolution of 10 km and 28 classes. The algorithm was applied to more than 20 years of resampled AVHRR monthly time series of reflectance, combined with one year of monthly Normalized Difference Vegetation Index (NDVI) from Spot Vegetation, mean annual rainfall, a forest cover map, and a Digital Elevation Model (DEM).

Since then, there have been many other notable attempts to provide information on irrigation from the regional to the continental/global scale. For instance, Ozdogan and Gutman [32] used a supervised classification to map the irrigated area in 2001 over the contiguous United States by using a combination of Landsat and MODIS data. Ambika et al. [34] developed yearly maps (2000–2015) of irrigated areas in India based on a thresholding of 16-day composite NDVI time series from MODIS. The decision tree between irrigated and non-irrigated areas was applied on each crop class (previously produced on the basis of IRS-P6) inside each agroecological zone. The following works of Meier et al. [35], Pervez and Brown [36], Zhu et al. [37], and Salmon et al. [38] provided some updates with respect to previous works by working on census areas rather than on crop classes. A notable example is the method applied by Peña-Arancibia et al. [31] on the Murray–Darling Basin in Australia, which used a supervised classification based on the random forest technique and data not only from vegetation (in this case, MODIS NDVI), but also from hydrometeorological data, such as monthly evapotranspiration (which was simply estimated by scaling Priestley–Taylor potential evapotranspiration, ETp, via a crop factor that was derived from other satellite observations) and monthly precipitation.

Later studies focused even more strongly on the synergistic use of machine learning methods and high-resolution remote sensing data. For instance, high spatio-temporal resolution NDVI data (30 × 30 m) from the Chinese HJ-1A/B (HuanJing, HJ) satellite were used by Jin et al. [39] to separate irrigated from rainfed areas in the semi-arid province of Shanxi in China, through a novel classification method based on a Support Vector Machine (SVM). They found that not only spatial but also temporal resolution may influence the classification results. A study by Chen et al. [40] also focused on a more extended irrigation detection which includes extracting frequency and timing information through data fusion of MODIS time series, Landsat OLI data, and ancillary data. The obtained fused Greenness Index (GI) estimates with an improved spatial resolution of 30 m were found to be effective in increasing the accuracy of irrigation mapping in the Gansu Province (China). Similarly, Ferrant et al. [41–43] have used a random forest classifier combining Sentinel-1 (S1) and Sentinel-2 (S2) data over southern India to investigate the advantages of high-spatial resolution and a multi-sensor approach. The input resolution allowed to retrieve irrigated areas for the two Indian climatic seasons at a resolution of 10 and 20 m.

Further studies highlighted both the need of sub-kilometric spatial resolutions to differentiate very fragmented irrigated areas and the need for combining multi-sensory information (in this case, radar for soil moisture and optical for vegetation) to better separate irrigated from non-irrigated land. For instance, Demarez et al. [44] applied an incremental random forest using a combination of optical (6 Landsat-8 bands each 16 days) and Synthetic Aperture Radar (SAR) data, revealing that the combined input improves the accuracy of the classification with respect to that performed with only one source. Similarly, Pageot et al. [45] used an approach that leveraged precipitation data, reaching a similar conclusion. They also revealed that the use of precipitation data improved the performance and that the aggregation of the high temporal resolution to monthly composites resulted in similar performances while reducing the calculation time.

The increasing availability of data, processing facilities, and novel classifiers also fostered data merging approaches, including modeled data from land surface and energy balance models for the detection of irrigated land. In the work of Deines et al. [29,46], the authors used a large number of variables derived from Landsat (9 in the first version, 11 in the second version) and more than 10 covariables, such as precipitation and slope, in a supervised classifier (CART and random forest) for classifying irrigated and non-irrigated areas. The different datasets were processed in the Google Earth Engine (GEE) computing platform, producing a classification at 30 m resolution claiming an overall accuracy above 95% of detected irrigation areas. Xu et al. [47] applied a similar approach in the subhumid temperate state of Michigan.

Besides machine learning, also more simple and "conceptual" approaches were developed based on the use of a mix of land surface and energy-balance model estimates and remote sensing variables. For instance, Zohaib et al. [48] looked at the biases between three modeled variables from the ERA-interim dataset (vegetation skin temperature, surface albedo, and soil moisture) and their corresponding variables derived from MODIS and ESA's Climate Change Initiative (CCI). McAllister et al. [49] exploited the fact that irrigated crops are supposed to be well-developed and colder than non-irrigated crops, and thus applied a simple threshold on NDVI and the difference of surface temperature to air temperature to detect irrigated areas. Similarly, Pun et al. [50] supposed that irrigated areas evaporate more than non-irrigated areas. Based on the Surface Energy Balance System (SEBS) model, they computed an evaporative fraction, and applied a simple threshold on vegetation indices and the evaporative fraction to discriminate irrigated areas.

3.1.2. Quantification Methods

Besides mapping irrigated areas, optical remote sensing can also offer some solutions for estimating the irrigation water use. Some of the approaches rely on calculating a crop coefficient and/or exploiting actual evapotranspiration (ET_a) estimates from remote sensing (e.g., MODIS, Landsat, S2, S3, VIIRS, and AVHRR). For example, Le Page et al. [15]

calculated the irrigation in the Tensift basin in Morocco as the difference between actual evapotranspiration and precipitation. They subtracted it from the known distributed water from dams to estimate the groundwater demand in an integrated modeling of demand and supply of water. This method exploited previous works on the determination of crop coefficients [51–59] to estimate actual evapotranspiration [60] by relying upon remote sensing-based vegetation indices [61–64]. The crop coefficient was also used as a supplement in a parameterized water balance approach by Saadi et al. [65] in order to show growth conditions.

Water and energy balance modeling approaches have also been investigated to assess irrigation water amounts using a combination of surface energy balance models and remote sensing data [66–68]. For instance, van Eekelen et al. [69] employed the surface energy balance algorithm for land (SEBAL, [70,71]) for mapping total ET_a, that is split into ET_a induced by precipitation (in rainfed agro-ecosystems) and ET_a induced by water withdrawals. Still based on ET, Hain et al. [72] compared the estimated ET_a by the Noah LSM (not incorporating irrigation) with a remotely sensed ET_a product retrieved using the Atmosphere-Land Exchange Inverse (ALEXI) model over Contiguous United States. The excess ET_a estimated by ALEXI was attributed to the irrigation. While large-scale irrigation agriculture could be mapped by this approach, the inherent error in Noah LSM and ALEXI ET_a estimates hindered the reliability of the method in certain parts of the study area. Conceptually similar was the work of Peña-Arancibia et al. [73], who used a combination of remotely sensed data and hydrological modeling outputs to estimate the volumes of water consumed in the form of evapotranspiration over irrigated lands in two sub-basins of the Murray-Darling basin (Australia). Alternatively, Olivera-Guerra et al. [74] used Landsat 7–8 Land Surface Temperature (LST) to derive a crop water stress coefficient that was injected directly into a water balance model, and then retrieved irrigation at the pixel scale before aggregating it to the plot scale. The method was tested on wheat fields in Morocco, exhibiting good performance for estimates of seasonal amounts, but lower agreement at the daily scale.

In an attempt at using only satellite-derived ET, Vogels et al. [75] compared the ET derived from the MODIS evapotranspiration product (MOD16A2) of natural and irrigated agricultural fields to calculate the excess water or recharge, which was used as an indicator for the water available for irrigation. Somewhat similar to the study of Vogels et al., and based on the research of van Eekelen et al. [69], advances have been made in developing irrigation quantification algorithms, specifically, the so-called "ETLook" algorithm [76]. Here, the similarity of natural and irrigated pixels is defined using multiple static sources, such as a land use map, a DEM, and soil type information. Maselli et al. [77] quantified irrigation amounts with the use of NDVI derived from S2 observations over a particularly complex mosaic of rainfed and irrigated crops in Central Italy, obtaining mean biases below 0.3 mm/day and 2.0 mm/week in two sites where irrigation reference data were available.

Lastly, Aragon et al. [78] investigated the capabilities of optical Leaf Area Index (LAI) derived from the novel Planet CubeSats constellation to estimate ET for irrigation quantification purposes using the Priestley–Taylor Jet Propulsion Laboratory (PT-JPL) retrieval model over a farm in an arid region of Saudi Arabia. In this case, 3 m spatial resolution ET retrievals were used to provide information on crop water use at the precision agricultural scale.

While the above-described methods that rely on optical satellite observations have yielded promising results for mapping irrigated areas, optical data are sensitive to weather conditions and cloud cover, which limits their utility in many tropical and temperate areas.

3.2. Microwave-Based Methods

Microwaves have the advantage that they are not hindered by weather conditions, and are independent of illumination. Microwaves are sensitive to the water content in the soil surface and vegetation and therefore have the potential to monitor changes in soil moisture as a result of irrigation events.

3.2.1. Mapping Methods

In recent years, microwave satellite soil moisture products have been introduced as a tool for detecting irrigated areas. One of the first studies was carried out by Kumar et al. [79], who compared the soil moisture distribution of a modeled dataset that does not incorporate irrigation information against various coarse spatial resolution satellite soil moisture products. Assuming that the satellite products do contain the irrigation signal, it can be expected that they will also exhibit wetter soil moisture conditions if irrigation is applied. The authors concluded that, even though promising results for the detection of irrigation were found in some specific areas, the spatial mismatch between model and satellite data as well as the confounding effects of topography, vegetation, frozen soils, and Radio Frequency Interference (RFI) led to substantial uncertainties in most regions. A similar approach has been used in several other studies in Spain [80], Australia and Morocco [81], and India [82]. Lawston et al. [83] further demonstrated that not only the spatial signature but also the seasonal timing of irrigation over three vastly irrigated areas in the United States could be identified using the Soil Moisture Active Passive (SMAP) enhanced 9 km product. In contrast, Fontanet et al. [84] found that disaggregated satellite soil moisture data obtained via the Disaggregation based on Physical and Theoretical Scale Change algorithm (DISPATCH) [85] is not sensitive to irrigation when it is applied locally, i.e., at spatial scales smaller than 1 km^2. Nevertheless, Dari et al. [86] showed the capability of DISPATCH downscaled Soil Moisture and Ocean Salinity (SMOS) and SMAP soil moisture data in detecting and mapping irrigation at 1 km spatial resolution over heavily irrigated portions of the Ebro River basin, in Spain.

In this context, SAR data seem to provide a new opportunity for mapping and monitoring irrigation at the agricultural field scale. Indeed, radar measurements are very sensitive to the soil water content due to the sharp increase of the soil dielectric constant associated with soil wetting. El Hajj et al. [87] observed this effect on irrigated grassland, showing a 1.4 dB increase of the radar signal observed by the TERRASAR-X sensor (X band), caused by irrigation applied one day before the satellite acquisition. The most important game changer of the recent years, in particular, has been S1, which brought about a strong increase in land use mapping methods in different climate contexts. The S1 satellite constellation (S1-A and S1-B) offers an unprecedented (for non-commercial satellites) data coverage with a time resolution of 6 days and a pixel size of 10×10 m in two polarizations, VV (vertically transmitted, vertically received) and VH (vertically transmitted, horizontally received), available free of cost. Different approaches have been proposed to map irrigated areas by considering the multi-temporal information from S1 backscatter observations to detect typical signal variations of irrigated areas [88–92]. Gao et al. [93] proposed an approach based on the direct analysis of the multi-temporal radar signal on each agricultural plot through different metrics (mean, standard deviation, correlation length, fractal dimension). This approach allowed the distinction of three classes, i.e., non-irrigated areas, irrigated crops, and irrigated trees with a precision of around 80% over a site in Catalonia (Spain). The same type of approach was tested with the temporal signal of soil moisture estimated from S1 data in a semi-arid zone in central Tunisia [92], achieving a relatively good accuracy. Bazzi et al. [94] proposed an approach that considers two different spatial scales for analyzing radar information in order to distinguish between irrigation and rainfall events. More specifically, the multi-temporal radar measurements are analyzed both at the agricultural plot scale and at a coarse 10 km scale. Through different techniques, such as principal component analysis and wavelet transformation, they achieved relatively high accuracies for identifying irrigated areas over a Catalonian site (Spain). Combining radar and optical observations using a random forest classifier improved their irrigation estimates even further. These good results based on S1 data have later been reproduced using a deep learning model to deal with the spatial transfer challenge for the mapping of irrigated areas [95].

S1 also enabled the retrieval of high-resolution soil moisture estimates, which are vital for irrigation management. Approaches are based on machine learning approaches,

including neural networks [88,89], change detection techniques [90,91], and also on direct inversion approaches of physical or semi-empirical models [92]. Typically, the estimates allow an accuracy of the order of 5% in volumetric soil moisture. Dari et al. [96] exploited plot-scale S1 soil moisture to map irrigation over an area in central Italy where agricultural fields are highly fragmented using a methodology based on statistical indices characterizing the spatio-temporal dynamics of soil moisture. The ability of microwave observation to retrieve irrigation timing information was also explored in some studies. Le Page et al. [16] proposed to assess irrigation timing at the plot scale by comparing the surface soil moisture of a model forced by crop coefficients derived from S2 to local surface soil moisture measurements and a soil moisture product derived from S1 [88]. The study was carried out over six maize plots in southwestern France and showed that the best retrieval of irrigation would be achieved with local measurements of surface soil moisture every 3–4 days. The authors also noticed that the technique is not adequate for the timing of small irrigation events (<10 mm) because of the 6-daily measurement frequency of S1, and that irrigation might be confused with rainfall events.

3.2.2. Quantification Methods

The quantification of the amount of water used for irrigation is generally more challenging than mapping the extent of irrigated areas alone. The first study trying to estimate the irrigation water amount from satellite soil moisture data has been carried out by Brocca et al. [97], who quantified irrigation at 9 pilot sites in the USA, Europe, Africa, and Australia, with 4 satellite soil moisture products. This study demonstrated the feasibility of such methods for the quantification of irrigation water amounts, especially when using satellite observations with low retrieval errors (<0.04 m^3/m^3) and short revisit times (<3 days). Good results were also found in regions with dry summers where the irrigation signal is more clearly pronounced (see Figure 2). The same approach was further applied by Jalilvand et al. [98], who obtained good agreement with ground-based irrigation data in a semi-arid region in Iran. Zhang et al. [99] qualitatively assessed the potential of various microwaved-based satellite soil moisture products for the detection of irrigation in China.
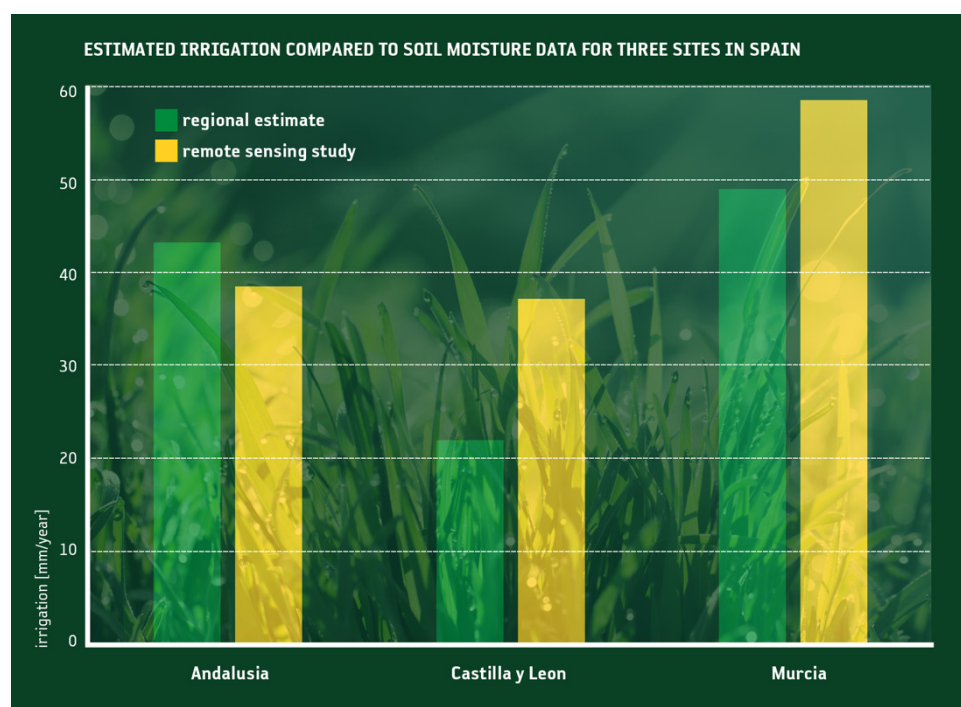

Figure 2. Comparison of observed (statistical survey) and estimated (through satellite soil moisture) annual irrigation volumes for three regions in Spain (adapted from Brocca et al. [97]).

An alternative method, but based on the same premise, i.e., that soil moisture predictions from (some) land surface models do not contain irrigated water, whereas satellite soil moisture retrievals do, was proposed by Zaussinger et al. [100], who estimated the irrigation water use over the Contiguous United States from various coarse-resolution sensors (ASCAT, SMAP, and AMSR2). This approaches the aggregated deviation between the modeled and satellite-observed soil moisture climatology as an irrigation water use estimate. A similar approach was employed by Zohaib and Choi [101] to identify trends of irrigation water amounts worldwide. Irrigation estimates from both studies showed a good correlation with country-level reported irrigation data, though irrigation was systematically underestimated. Notwithstanding the potential of currently available microwave-based soil moisture products, their biggest limitation to the retrieval of accurate irrigation water amounts is the coarse spatial resolution of (most) sensors, i.e., pixel sizes in the order of tens of km. To address this issue, Dari et al. [102] recently exploited 1 km DISPATCH downscaled versions of SMOS and SMAP soil moisture to estimate almost 7 years of irrigation water amounts over an intensely irrigated area in the North East of Spain. Irrigation was retrieved through an improved version of the SM2RAIN algorithm, in which the crop evapotranspiration was estimated according to the FAO model. Comparisons with district-scale benchmark irrigation volumes showed the suitability of the method to estimate actual irrigation amounts, as well as the skill in reproducing the temporal dynamics of irrigation. Zappa et al. [103] developed a framework for the detection and quantification of irrigation based on the TU-Wien S1 soil moisture product at 500 m resolution [91]. Good agreement was found against field-scale irrigation reference data in Northern Germany, both in terms of spatial patterns and temporal dynamics. However, the overall irrigation volumes were generally underestimated as a result of field-specific irrigation systems and management practices, and the longer revisit time of the S1 images (up to a few days) compared to coarse-scale products.

3.3. Gravimetry-Based Methods

While multispectral-based and microwave-based methods rely on remotely sensed estimates of quantities that are driven directly by irrigation (e.g., the soil water content or vegetation transpiration), gravimetric remote sensing may bear more indirect irrigation information. Specifically, gravimetric measurements have been used to derive so-called terrestrial water storage (TWS), which are temporally averaged (typically monthly) water mass change observations of anomalies of the total mass of water stored on and beneath the land surface. Temporal trends in TWS from GRACE data [104,105], for instance, have been linked to heavily irrigated regions of the world caused by human-induced (irrigation) groundwater depletion (e.g., [106]).

The largest caveat of gravimetric remote sensing, however, is its coarse horizontal resolution, which is about 300 km at mid-latitudes [107]. TWS retrievals, therefore, contain many other confounding factors (such as snow, surface water in lakes and rivers, etc.) that need to be removed when attempting to link TWS anomalies to groundwater depletion from irrigation.

4. Irrigation Modeling and Data Assimilation

Irrigation modeling (i.e., providing models with tools to simulate irrigation) is a way to simulate the additional water applied on soils from internal or external sources (such as canals, groundwater, or pipelines). However, the reliability of the irrigation schemes used in hydrological, land surface, or crop models depends on the validity of a number of simplifying assumptions and input parameters. For example, irrigation water is often applied to the land surface only when soil moisture drops below arbitrarily chosen soil moisture thresholds in order to restore optimal growing conditions. These thresholds typically depend on soil and vegetation parameters, which in turn depend on large-scale soil texture maps. For example, Kueppers et al. [108] and Lobell et al. [109] have set a critical value for the root-zone soil moisture (RZSM) within irrigated tiles based exclusively

on the soil field capacity. Given the simplicity of these methods, both the timing and amount of such irrigation estimates can be very inaccurate as they assume that water resources are unlimited, and that the farmer's irrigation decision is based on soil water availability only. In reality, several other factors are considered, including specific practices such as soil leaching, water regulations, climate, and resource availability.

In the recent years, the irrigation parameterization in large-scale Land Surface Models (LSMs) has seen considerable improvements owing to the development of more complex irrigation schemes [110]. For instance, Ozdogan et al. [111] included three trigger criteria to dynamically simulate daily irrigation in the Noah LSM [112], which are: (i) whether a tile is potentially irrigated, (ii) whether it is the growing season (defined by a threshold of 40% of annual range of greenness fraction), and (iii) how much water is available (or more importantly, lacking) in the root zone. In this scheme, irrigation is applied as additional precipitation when the RZSM falls below a triggering user-defined threshold until the field capacity is reached. Additional improvements in irrigation parameterization have been made by implementing various types of irrigation systems. The Noah LSM, for example, can be coupled with a drip as well as with a flood method (both built based on the work by Evans and Zaitchik [113]). These two additional schemes, characterized by differences in frequency, timing, and amount of irrigation, are described by Lawston et al. [114]. Some studies have also attempted to incorporate irrigation schemes into other global LSMs, including the Community Land Model (CLM, [115]) and the Organizing Carbon and Hydrology in Dynamic Ecosystems (ORCHIDEE) model [116], demonstrating that intensive irrigation at the regional scale strongly affects river discharge and groundwater and has a regional impact on the partition of energy between sensible and latent fluxes. Despite these developments, however, irrigation modeling is still in its infancy and still prone to uncertainties.

A potential remedy to model uncertainties due to missing or inaccurately modeled irrigation might be data assimilation. For example, Girotto et al. [117] investigated the extent to which GRACE TWS data assimilation in the Catchment Land Surface Model (CLSM) could correct for errors due to missing model processes such as groundwater extraction for irrigation. However, even though the satellite data assimilation largely improved the estimation of some processes, it also deteriorated the estimates of others due to inappropriate treatment of the irrigation water source. To reconcile the information contained in GRACE with LSM simulations, Nie et al. [118] modified the Noah-MP LSM in a study over the High Plains Aquifer (HPA) to include a dedicated groundwater-based irrigation scheme. Additionally, to account for seasonal and interannual variability in irrigated areas, the authors applied a monthly time-varying greenness vegetation fraction (GVF) dataset within the model. In a successive study, Nie et al. [119] assimilated GRACE TWS into the Noah-MP LSM with and without an irrigation scheme activated over the HPA, and found that the best overall performance was, over most of the study region, obtained when the data assimilation system was indeed coupled with the irrigation scheme.

The inclusion of irrigation in land surface modeling, either by direct irrigation modeling alone or facilitated by data assimilation, is not only important to obtain consistent and accurate land surface estimates, but also to improve atmospheric and climate simulations. A wide range of studies assessing the irrigation effects on climate have focused on daily/annual irrigation amounts (e.g., [120–122]) or on evapotranspiration fluxes due to irrigation (e.g., [123]) as climate model input. Lawston et al. [114] used the Land Information System (LIS) together with the NASA Unified Weather Research and Forecasting Model (NU-WRF) framework to investigate the effects of drip, flood, and sprinkler irrigation methods on land–atmosphere interactions, including land–planet boundary layer coupling and feedbacks at the local scale. Overall, outcomes from LSM studies have shown that irrigation increases SM, leading to greater evapotranspiration with increases in latent heat flux and decreases in both sensible heat flux and coupling between SM and latent heat flux in water-limited environments (e.g., [111,124–126]). This repartitioning of the surface

energy and water balance causes lower surface air temperature and elevated atmospheric water vapor that contributes to the greenhouse effect [9,111,114,125].

However, since the primary purpose of these coupled models is to study land–atmosphere interactions, LSM irrigation schemes generally ignore the source of water that is applied as irrigation and do not account for the impact that withdrawals have on groundwater or surface water processes. This may suffice when estimating on-field consumptive water use [111,127,128] or studying land–atmosphere interactions [113,114,129], but it prevents the application of these models to integrated water resource analysis or to evaluate trends in water storage [130]. In contrast, hydrological models have been developed in response to global water scarcity concerns, thus they tend to better represent human-driven hydrological processes such as irrigation [131]. Examples of such regional and global models include the WaterGAP model [132], or the WBMplus model [133]. While these models too may benefit from (irrigation) data assimilation, such studies are still pending.

5. The User Perspective: Observation Requirements and Current Obstacles

From a practical point of view, it is still not evident whether irrigation information collected from satellite observations, models, and their combinations can help farmers, water managers, or basin authorities. Recent important contributions highlight that this information is paramount for an efficient water and agricultural management, especially over data-scarce regions [134]. Notable examples derive from irrigation monitoring systems platforms, for instance the WUEMOCA project developed by the University of Wuerzburg, Germany [135], or the FAO's portal to monitor Water Productivity through Open-access of Remotely sensed derived data (WaPOR), which promote the use of satellite data to help countries monitor agricultural water productivity, identify water productivity gaps, and find solutions [136].

This section aims to understand the potential utility of EO-based irrigation information for users. To that end, we reviewed the answers of a survey that has been conducted with a set of ten users, representative of different Mediterranean countries (Ebro River basin in Spain, the South of France, Po River Valley and Sardinia, in Italy). We did not expect the users to have knowledge of remote sensing capabilities, but this was considered advantageous as we were interested in understanding their real needs and the potential utility of current and future satellite mission to satisfy these needs.

This survey is not comprehensive and does not aim to picture farmer requirements worldwide, but aims at fostering the discussion on whether the satellite-based information on irrigation is mature enough to be used in a challenging area such as the Mediterranean region. Therefore, it must be interpreted only in a qualitative sense. Nevertheless, even though the discussion focuses on the Mediterranean, findings might likely be transferrable to other areas. A few limitations shall be noted upfront, however: The utility of remote sensing for irrigation monitoring and management might depend on many factors, such as the type of user and its responsibilities (basin authority, which manages a very large hydrological unit; irrigation district, which distributes water to the farmers; large farming enterprise, which may have access to modern technology to manage the farm; small farmer, with limited access to technology), the spatial organization of the irrigation fields (size of the fields, size of the properties, diversity or homogeneity of cropping patterns), the type of irrigation method (modernized or traditional, localized or extensive), the cost of water (price of water, price of energy, contribution to the maintenance of the infrastructure), etc. Thus, the requirements are very heterogeneous, and potential irrigation products must be able to provide information to a wide array of users with very different needs in terms of spatial resolution and temporal frequency, and latency of observations, type of information and variables, accuracy, and accessibility.

In the following, we review each of these factors and discuss the answers provided by contacted users and organizations in relation to the ability of remote sensing observations

to track and detect irrigation. The used questionnaire, which is part of the Irrigation+ project funded by the European Space Agency (ESA) (See supplementary Material).

5.1. User Characteristics

The majority of the contributing organizations belong to an irrigation district or irrigation consortia (7/10), that is, they are farmers or institutions that directly serve the farmers managing or distributing water. The remainder of them were public actors, such as basin authorities or other irrigation-related public actors, who are less focused on the actual distribution of water but are interested in managing and accounting for the whole hydrological cycle of a large area (e.g., a river basin).

The size and spatial structure of the irrigated fields and irrigation districts in Mediterranean areas are often tied to complex historical and technical processes. For example, in the Po River valley (Italy), this condition has historical reasons related to the Roman centuriation, where the divisions of the land were based on the needs and technical limitations of the ancient society (see Figure 3). In other countries, this might have changed with time due to the influence of the Post-Roman occupation of the land and to the current need to facilitate agricultural practices and to boost production. For instance, in Catalonia (Spain), in modernized irrigation areas, land is often reorganized to ensure a more homogeneous division and thus agricultural plots tend to have larger extents than they used to have, when traditional irrigation methods were used.
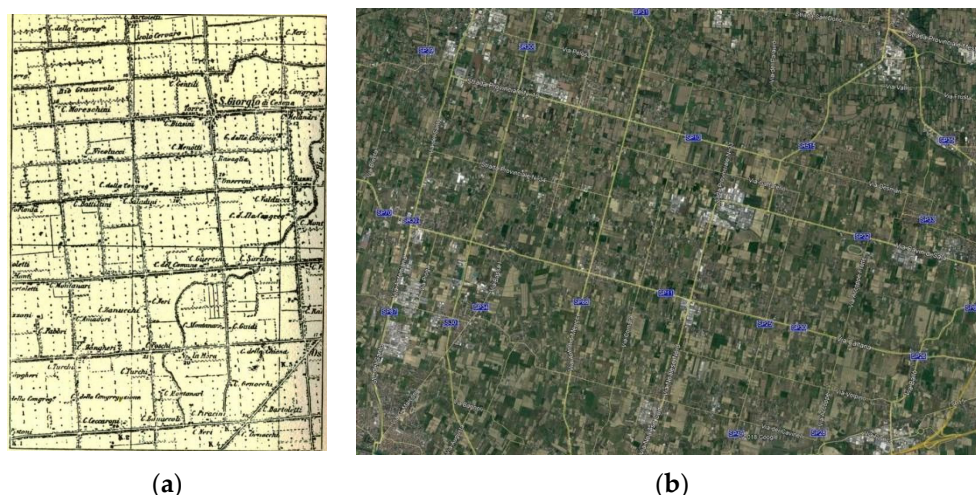

| (**a**) | (**b**) |

Figure 3. Centuriation near Cesena, Italy, in a late nineteenth century Italian military map—Roman grid system (**a**) and what is left today in the Po River valley with superimposition of the old system (**b**). Source: Wikipedia (https://en.wikipedia.org/wiki/Centuriation (accessed on 13 October 2021)).

Despite the change of land use in Europe, the irrigation districts and consortia tend to be organized in many small fields (although this varies from country to country) relative to the size of a satellite footprint. These fields might contain different types of crops close to each other and may use different irrigation systems, which complicate attempts to stratify them based on crop type or the type of irrigation. Furthermore, water use exhibits large field-to-field variability, which cannot be explained fully by differences in weather, soil type, crop choice, or technology [18], but instead depends largely on the farming practices adopted by different farmers.

The majority of the contacted organizations have mixed systems. For example, it is not uncommon to grow fruit trees, which often use drip irrigation, close to maize fields that will probably use sprinklers. This highlights that collecting irrigation information can be very challenging with only one type of observation, and combining multiple techniques to retrieve information about irrigation (i.e., thermal, optical, and microwave) may be advantageous.

Concerning the technique used to measure irrigation, the majority of the interviewees stated that the amount of water applied is not measured directly in the field but with water meters placed in the main canal or pipeline, or as a total volume of water extracted from wells. Only two interviewees answered that they check soil status in person or use a rain gauge placed in the field to check the accumulated irrigation at the end of the year. The provided answers demonstrate that the collection of in situ irrigation data can be subject to substantial uncertainties, as also highlighted by Foster et al. [137].

Moreover, as the majority of the interviewees measure irrigation at the entrance of the irrigation district, identifying the plot actually irrigated can be very challenging, especially for the basin authorities who, often, do not have access to the counters. This is a very common situation over developing regions and in many places over the Mediterranean basin. Current pressures (the need to increase production and economic viability of farming activities and the inability to increase the offer, e.g., dams, and the impacts of climate change on the overall water resources' availability) are pushing towards pervasive modernization of irrigation, with drip irrigation being the method with a faster increase in use [138], so the situation will likely change in the near future.

5.2. Current Practices Versus Current Satellite Capabilities

5.2.1. Management Systems

To understand to what degree satellite observations can help in the monitoring and the management of irrigation, we first asked the organizations whether they are already using any system for the management and measurement of irrigation applications. The answers varied from no system at all to fully automated, remotely controlled systems. Of those who do use management systems, most use point-scale in situ soil moisture measurements, while nobody mentioned the use of remote sensing observations. Furthermore, sometimes, there are in situ measurements that are not accessible to some stakeholders. For instance, the basin authority may not have access to the existing water accounting system within the irrigation district (they just track what has been delivered through the main canal). Additionally, there can be illegal uses of irrigation water that are unmetered. This happens in some Mediterranean areas [139] and remote sensing can play an important role in quantifying these water withdrawals. In summary, we believe that there is space for remote sensing observations and methods that integrate remote sensing information to provide useful tools for optimal irrigation and water resource management.

5.2.2. Irrigation Strategies

When asked about the number of irrigation applications, the answers ranged from 2 to 30 irrigation applications per month. We also asked about a typical crop they refer to, but no answer was provided. This probably highlights the difficulty in the control of irrigation on single fields or areas where specific crops are grown. Another complicating factor is crop rotation (i.e., crop types might change from year to year), which might also depend on the very uncertain forecast of water resources for that year [140]. Farmers may also change the size of the irrigated surface, the crop, the number of harvests per season, and so on. Accordingly, the irrigation strategy may change for each field and each year. The amount of irrigation applications is central to understanding the importance of the revisit time of the sensors used to retrieve information about irrigation. With 30 irrigation applications per month (i.e., once per day), it is very likely that products characterized by a temporal resolution of 2–3 days will miss irrigation events. On the other hand, both techniques based on soil moisture and evapotranspiration provide an indirect detection and quantification of irrigation exploiting the memory of the soil moisture and evapotranspiration signals. That is, if water is applied in the morning, the process of transpiration does not interrupt instantaneously and might continue as long as the water is available and the plant is able to transpire it. As a secondary effect, this determines a soil moisture depletion which is also visible after the satellite passes.

5.2.3. Employed Technology

The employed irrigation method determines the potential ability of the techniques described in Section 3 to detect and quantify irrigation. For instance, sprinkler and flooding/gravity types of irrigation systems cause significant (surface) soil wetting, which translates into a strong response of the remotely sensed signal. This facilitates irrigation detection and quantification with soil moisture-based techniques. In contrast, drip irrigation systems apply much smaller water amounts, whose detection can be very challenging, especially for coarse-resolution satellite sensors. In this case, evapotranspiration-based techniques (based on the use of thermal sensors) can provide better performance as the actual ET rate for crops located in a drip-irrigated field can be very close to their potential ET, which is generally not the case for non-irrigated crops. Moreover, thermal-based methods to retrieve evapotranspiration have the advantage of a higher spatial resolution suitable for the monitoring of small-scale fields, where drip irrigation is also more commonly used. Nevertheless, this is at the expense of the revisit time, reaching at best 8 days by combining Landsat-7 and -8 with the sensors currently in orbit. A significant way to reduce the revisit time could derive from the future satellite missions, such as Thermal InfraRed Imaging Satellite for High-resolution Natural resource Assessment (TRISHNA, [141]), a future high-resolution space-time mission in the thermal infrared (TIR) led jointly by the French (CNES) and the Indian (ISRO) space agencies for a launch planned in 2025, or by the high-priority candidate mission High Spatio-Temporal Resolution Land Surface Temperature Monitoring Mission (LSTM, [142]), which will provide enhanced measurements of land surface temperature with a focus on responding to user requirements related to agricultural monitoring.

Other than the type of irrigation system, its relation to the farmer organizations can play a role. For instance, in traditional flood irrigation, irrigation is performed in turns, so there are a few events each month. With modern systems, such as sprinklers, irrigation can take place every day in order to compensate for water deficits caused by plant transpiration and soil evaporation. However, this also depends on the objectives of the farmers, as the different strategies lead to different quantities and qualities of the product and the farmers may bet on quality or quantity depending on the year. Therefore, the frequency is often tied to the irrigation method, but the relationship is not univocal. In summary, with traditional irrigation methods, the required temporal resolution to obtain information on irrigation can be larger than 1–2 days, whereas with modern systems (i.e., sprinkler), daily temporal resolution is needed. Furthermore, with modern systems that use daily irrigation, soil moisture will tend to be more constant than with classical irrigation systems, and techniques relying solely on soil moisture for the retrieval of irrigation amount might be suboptimal. With traditional systems, due to the turn-like method of irrigation, soil moisture will be more variable and will alternately increase and decrease depending upon whether irrigation will or will not take place, so techniques which exploit soil moisture for the retrieval of irrigation might provide better performance.

Despite the limitations and difficulties in estimating irrigation from remote sensing observations, where the technical advancement is still low (e.g., Urgell area in Spain and developing countries) and the possibility to measure irrigation is very scarce as no counter nor modern irrigation systems exist to measure water in the soils, satellite data can be very important. This is also perceived by users, as there seems to be a growing interest in the use of remote sensing products to better plan and manage irrigation.

5.3. Operational Observation Requirements

In this section, we aim at understanding the current gap between the existing capabilities of satellite observations to observe soil moisture, evapotranspiration, and information on irrigation and the real needs of the users. The discussion is based on the reviewed literature from Section 3 and the questionnaire implemented.

A general issue is the fact that satellites can provide only information on the few first centimeters of the soil, whereas information on the root zone soil moisture (0–100 cm) is

most important for the crops and hence most desired by users. While this information cannot be directly obtained from satellites, models can be integrated with observations to provide information of the water stored in the root zone. Based on the size of the agricultural fields in the Mediterranean, the spatial resolution at which remote sensing products should provide information on irrigation is below 1 km (10–100 m for most of the users). This of course represents a big challenge for the current state of the satellite missions. Currently, microwave data from S1, S2, and Landsat-8 could indeed meet these needs and models too can run at these spatial resolutions, assimilating satellite data with a spatial support larger than/equal to 1 km to correct states and fluxes at smaller spatial scales, providing information on irrigation. There is thus a realistic potential to cover the desired spatial scales identified by the users. Concerning the temporal resolution, 1–7 days is the desired window for farmers, while for basin authorities, monthly to seasonal scales seem to be sufficient. Even though current satellite missions cannot provide retrievals of irrigation information with daily temporal resolution at a spatial resolution of 10 m, weekly estimates at a resolution of 100 m–1 km are indeed realistic.

Concerning the spatial resolution of evapotranspiration data, the requirements are similar to the one of soil moisture with values below 1 km for farmers and above for basin authorities interested in water management. Overall, the spatial/temporal resolution of 100–500 m daily can theoretically be provided from satellites, for example from MODIS observations, while lower spatial resolution could be obtained with Landsat [143] and the new Sentinel satellites [144]. In addition, models can run at this resolution and can benefit from the assimilation of satellite soil moisture/backscatter from S1 data or by LST information from thermal sensors [127].

Regarding the desired accuracy (i.e., the difference between the estimated and true irrigation volumes) of the irrigation data, it seems that a value below 30% would be desired (based on the answers of the farmers). However, due to the lack of reliable ground reference information about irrigation, it currently remains difficult to provide exact accuracy estimates. Nevertheless, in a recent study, Dari et al. [102] reported irrigation retrieval accuracies that span from 10% to 40%, which is not far from the defined targets.

6. Synthesis and Future Perspectives

This study provided a comprehensive review of the use of remote technologies to retrieve information on irrigation, and methods to integrate this information with models. Moreover, we assessed whether this information meets the requirements of various actors working in the field of water resource management and agriculture. What emerged from the literature is synthetized below:

(1)   The information of irrigation collected in situ is very limited due to the reluctance of farmers and managers to share these data [137], and the difficulty to collect data at global and regional levels. This poses a big challenge for the understanding of energy, water, and carbon cycles, climate interactions and future projections, sustainable agriculture and water management, food production, and water security.

(2)   Estimates of areas equipped for irrigation, derived from inventories of national and local authorities, have partially covered this gap, but being mainly based on statistics and sparsely and historically collected information, they are likely to be inaccurate and inhomogeneous. Moreover, this information is static and thus does not say when, where, and how much irrigation has been applied. Despite these limitations, these data remain a reference for many applications, including global hydrological modeling, modeling of changes in crop productivity, or climate impact assessments.

(3)   In the last twenty years, there has been a substantial improvement in both spectral, spatial, and temporal resolution of Earth observations, which has boosted methodological developments. A first advance was to separate the identification of irrigated areas from general land cover classification approaches. A second advance came with improvements in spatial resolution, which allowed for more accurate assessments of irrigated areas [123,145] that do not hinge on information about the fraction of

irrigated area within low-resolution pixels. A third advance was the synergetic use of various satellite, climatic, and ecoregions time series instead of vegetation index time series alone.

(4) The automation of high-resolution time series processing has benefited greatly from the emergence of platforms that allow the parallel processing of big amounts of data, such as Google Earth Engine, Amazon, or the European DIAS. The technological advances have made it feasible to estimate the irrigated area at ever smaller time steps, progressing from a decadal overview of the areas equipped for irrigation toward the actual irrigated area at the beginning of the season, also thanks to the continuous development of new machine learning and classification methods which so far relied mainly upon supervised types of algorithms. The lack of the real data to guide these algorithms, especially over data-scarce regions, surely demands for a more massive use of unsupervised techniques [146,147].

(5) Microwave-based observations and their combination with optical data and models have provided new ways to map irrigated areas. Previous work using coarse-scale and disaggregated soil moisture products have shown potential for retrieving information of irrigation from space, but also have several limitations associated with: (i) the noise of these products compared to the strength of the irrigation signal, and (ii) the scale mismatch between the satellite footprint and the size of the irrigated fields. In this context, SAR data have demonstrated to be a viable way to provide information on irrigation mapping and researchers are currently exploring ways to retrieve quantitative irrigation estimates from them as well. The latter is, however, more challenging compared to simple irrigated area mapping.

(6) Visible, near-infrared, and microwave-based methods have all demonstrated a certain ability to quantify volumes of applied irrigation. However, VNIR observations—besides their inherent limitations due to cloud cover—can theoretically only provide the consumptive water use (i.e., the amount of water that is transpired by the crop and evaporated from the soil), and thus neglect the amount of water infiltrating to the subsurface, or MW observations have been demonstrated to be sensitive to noise and vegetation as well as to the satellite revisit time. Indeed, the temporal frequency is a crucial factor to reproduce the spatio-temporal dynamics of irrigation. In fact, the irrigation frequency depends on many factors (e.g., climatic conditions, crop type, water availability) and low-frequency data are often not able to detect irrigation events occurring at a not-negligible time distance from the acquisition.

(7) Hardly affected by surface conditions, gravimetric measurements derived from GRACE and its successor GRACE-FO could provide important information on irrigation, but the spatial and temporal resolution achievable with these instruments have so far limited their application to only very large areas.

(8) Most studies addressing the quantification of irrigation have employed modeling components, which potentially exhibit large uncertainties due to the need of a suitable parameterization and high-quality input observations (especially land cover and soil maps in land surface and hydrological models). For instance, the means of irrigation (i.e., sprinkler, drip, or flood) strongly affects the daily timing and quantity of irrigation water applied, while input data providing information on irrigated areas and starting of the growing season are required but rarely available. Additionally, modeled irrigation schemes generally ignore the source of applied water (i.e., surface water or groundwater), thus not allowing an integrated water resource analysis.

(9) Considering that there has been increasing interest in understanding both the role of the irrigation on land–atmosphere interactions [148] and the impact of irrigation on water resources [149], coupling remote sensing information with land surface models for an improved representation of anthropogenic activities seems to be a key challenge to be addressed in the near future (e.g., [119,150]).

Notwithstanding the importance of the studies in irrigation retrieval research and its representation in Land Surface Models and Hydrological models to advance the knowledge

of its impact on the climate and land systems, quantification, timing, and mapping of irrigation have a paramount importance also for agricultural and operational water resource management, where a plethora of actors are involved with very different needs. The scales of action are therefore very diverse, as are the capabilities of the different available satellite missions (see Table 2).

Table 2. Potential of satellite-based remote sensing observations to detect irrigation information from space as a function of the scale of application.

	Irrigation Mapping	Irrigation Quantity	Irrigation Timing
Products at local/field scale in support of water management and agriculture (approx. <100 m)	With SAR and thermal data (up to 30 m with Landsat and S2-S3, 10–100 m with SAR S1 data)	Up to 10–100 m with SAR data and 30 m with visible and near-infrared sensors. Accuracy limited by the temporal resolution of the sensors and noise.	With SAR and thermal and optical data depending on the location. Limited to temporal resolution larger than a day.
Products at national/basin scale in support of water management (500 m–1 km)	With SAR (e.g., S1) and thermal data (e.g., MODIS, S2–S3) and their combination. Suitable for relatively large agricultural areas	With SAR (e.g., S1) and thermal data (e.g., MODIS, Landsat, S2, S3) and their combination. Accuracy depends upon satellite revisit time and noise. Cloud cover can be an issue.	Daily with thermal data (e.g., MODIS). Weekly and sub-weekly with SAR depending on the location and other visible and near-infrared observations such as S2 and S3 depending on the cloud cover.
Products at regional/global level (>10 km)	With active and passive coarse-scale microwave observations limited to large and intensive irrigated areas much larger than the product spatial resolution (large and intensively irrigated areas of India, USA, China, Brazil). With any optical, near-infrared sensor	With active and passive coarse-scale microwave observations, limited to large and intensive irrigated areas much larger than the product spatial resolution. Noise can be an issue. With any visible and near-infrared sensor. Gravimetric measurements (GRACE).	With coarse-scale microwave observations, potentially daily if the signal is sufficiently strong with respect to the noise and with thermal data.

Improving the efficiency of water use by agriculture and predicting the impacts on the different reservoirs requires the knowledge of irrigation water inputs and timing at the decision-making scales: (1) the plot/day for the farmer interested in irrigation scheduling on a day-to-day basis, (2) the irrigated perimeter/month for the irrigation district to help in the water distribution to farmers, and (3) the watershed/season for the manager for land use planning. For these scales, the different requirements have to face the diverse geographic/historical/cultural/economic conditions of the regions, which change over time, and the maturity of the technological advancement of satellite observations. There are many missions planned for the future which will help to fill these gaps.

A potential benefit for irrigation retrieval could be derived from the Global Navigation Satellite System Reflectometry (GNSS-R) mission, such as the NASA Cyclone Global Navigation Satellite System (CYGNSS) [151,152], and from the US-Indian NASA-ISRO SAR (NISAR) and Radar Observing System for Europe—L-band (ROSE-L) SAR missions [153],

planned to be launched in 2022 and 2028, and that should provide improved soil moisture estimates over vegetated areas and from a deeper soil layer compared to C-Band (S1) products at higher spatial resolutions. In addition, higher temporal resolution can be achieved with a constellation of low-cost CubeSats with a GNSS reflectometer onboard. Other missions such as TRISHNA and ESA LSTM missions already mentioned above will provide enhanced high spatial-temporal resolution measurements of land surface temperature, which would be helpful to map small irrigated fields. These missions, among others already planned, should cover the majority of the users' requirements at scales identified in Table 2, and that should bring important progress to the land and water management with significant benefits for food and water security.

References

1. FAO 2016. AQUASTAT Database. Available online: https://www.fao.org/aquastat/en/ (accessed on 29 July 2021).
2. Gleick, P.H.; Allen, L.; Christian-Smith, J.; Cohen, M.J.; Cooley, H.; Heberger, M.; Eli Moore, E.; Morrison, J.; Orr, S.; Schulte, P.; et al. *The World's Water: The Biennial Report on Freshwater Resources*; Island Press: Washington, DC, USA, 2012.
3. Foley, J.A.; Ramankutty, N.; Brauman, K.A.; Cassidy, E.S.; Gerber, J.S.; Johnston, M.; Mueller, N.D.; O'Cinnell, C.; Ray, D.K.; West, P.C.; et al. Solutions for a cultivated planet. *Nature* **2011**, *478*, 337–342. [CrossRef] [PubMed]
4. Ozdogan, M.; Yang, Y.; Allez, G.; Cervantes, C. Remote sensing of irrigated agriculture: Opportunities and challenges. *Remote Sens.* **2010**, *2*, 2274–2304. [CrossRef]
5. Matthews, O.P.; Germain, D.S. Boundaries and transboundary water conflicts. *J. Water Resour. Plan. Manag.* **2007**, *133*, 386–396. [CrossRef]
6. Fader, M.; Shi, S.; von Bloh, W.; Bondeau, A.; Cramer, W. Mediterranean irrigation under climate change: More efficient irrigation needed to compensate for increases in irrigation water requirements. *Hydrol. Earth Syst. Sci.* **2016**, *20*, 953–973. [CrossRef]

7. Tramblay, Y.; Llasat, M.C.; Randin, C.; Coppola, E. Climate change impacts on water resources in the Mediterranean. *Reg. Environ. Chang.* **2020**, *20*, 83. [CrossRef]

8. Rosa, L.; Chiarelli, D.D.; Sangiorgio, M.; Beltran-Peña, A.A.; Rulli, M.C.; D'Odorico, P.; Fung, I. Potential for sustainable irrigation expansion in a 3 °C warmer climate. *Proc. Natl. Acad. Sci. USA* **2020**, *117*, 29526–29534. [CrossRef]

9. Döll, P.; Siebert, S. Global modelling of irrigation water requirements. *Water Resour. Res.* **2002**, *38*, 8.1–8.10. [CrossRef]

10. Vörösmarty, C.J.; Green, P.; Salisbury, J.; Lammers, R.B. Global water resources: Vulnerability from climate change and population growth. *Science* **2000**, *289*, 284–288. [CrossRef]

11. Alter, R.E.; Im, E.S.; Eltahir, E.A. Rainfall consistently enhanced around the Gezira Scheme in East Africa due to irrigation. *Nat. Geosci.* **2015**, *8*, 763–767. [CrossRef]

12. Haddeland, I.; Skaugen, T.; Lettenmaier, D.P. Hydrologic effects of land and water management in North America and Asia: 1700–1992. *Hydrol. Earth Syst. Sci.* **2007**, *11*, 1035–1045. [CrossRef]

13. Breña-Naranjo, J.A.; Kendall, A.D.; Hyndman, D.W. Improved methods for satellite-based groundwater storage estimates: A decade of monitoring the high plains aquifer from space and ground observations. *Geophys. Res. Lett.* **2014**, *41*, 6167–6173. [CrossRef]

14. Hu, X.; Shi, L.; Zeng, J.; Yang, J.; Zha, Y.; Yao, Y.; Cao, G. Estimation of actual irrigation amount and its impact on groundwater depletion: A case study in the Hebei Plain, China. *J. Hydrol.* **2016**, *543*, 433–449. [CrossRef]

15. Le Page, M.; Berjamy, B.; Fakir, Y.; Bourgin, F.; Jarlan, L.; Abourida, A.; Benrhamen, M.; Jacob, G.; Huber, M.; Sghrer, F.; et al. An integrated DSS for groundwater management based on remote sensing. the case of a semi-arid aquifer in morocco. *Water Resour. Manag.* **2012**, *26*, 3209–3230. [CrossRef]

16. Le Page, M.; Jarlan, L.; El Hajj, M.M.; Zribi, M.; Baghdadi, N.; Boone, A. Potential for the detection of irrigation events on maize plots using sentinel-1 soil moisture products. *Remote Sens.* **2020**, *12*, 1621. [CrossRef]

17. Bretreger, D.; Yeo, I.-Y.; Hancock, G.; Willgoose, G. Monitoring irrigation using landsat observations and climate data over regional scales in the Murray-Darling Basin. *J. Hydrol.* **2020**, *590*, 125356. [CrossRef]

18. Foster, T.; Gonçalves, I.Z.; Campos, I.; Neale, C.M.U.; Brozović, N. Assessing landscape scale heterogeneity in irrigation water use with remote sensing and in situ monitoring. *Environ. Res. Lett.* **2019**, *14*, 024004. [CrossRef]

19. OECD. *Drying Wells, Rising Stakes: Towards Sustainable Agricultural Ground-Water Use*; OECD: Paris, France, 2015.

20. Copernicus—The European Earth Observation Programme. Available online: https://ec.europa.eu/growth/sectors/space/copernicus_en (accessed on 29 July 2021).

21. Bartholomé, E.; Belward, A.S. GLC2000: A new approach to global land cover mapping from Earth observation data. *Int. J. Remote Sens.* **2005**, *26*, 1959–1977. [CrossRef]

22. Tateishi, R.; Zhu, L.; Sato, H.P. GLC2000 Database. The Land Cover Map for Central Asia for the Year 2000. European Commision Joint Research Centre. 2003. Available online: https://forobs.jrc.ec.europa.eu/products/glc2000/publications.php (accessed on 13 October 2021).

23. Thenkabail, P.S.; Biradar, C.M.; Turral, H.; Noojipady, P.; Li, Y.J.; Vithanage, J.; Dheeravath, V.; Velpuri, M.; Schull, M.; Cai, X.L.; et al. *An Irrigateed Area Map of the World (1999) Derived from Remote Sensing*; Research Report 105; International Water Management Institute: Colombo, Sri Lanka, 2006.

24. ESA. Land Cover CCI Product User Guide Version 2. *Tech. Rep.* **2017**. Available online: Maps.elie.ucl.ac.be/CCI/viewer/download/ESACCI-LC-Ph2-PUGv2_2.0.pdf (accessed on 13 October 2021).

25. Portmann, F.T.; Siebert, S.; Döll, P. MIRCA2000-Global monthly irrigated and rainfed crop areas around the year 2000: A new high-resolution data set for agricultural and hydrological modeling. *Glob. Biogeochem. Cycles* **2010**, *24*, GB1011. [CrossRef]

26. Siebert, S.; Kummu, M.; Porkka, M.; Döll, P.; Ramankutty, N.; Scanlon, B.R. A global data set of the extent of irrigated land from 1900 to 2005. *Hydrol. Earth Syst. Sci.* **2015**, *19*, 1521–1545. [CrossRef]

27. Siebert, S.; Döll, P.; Hoogeveen, J.; Faures, J.-M.; Frenken, K.; Feick, S. Development and validation of the global map of irrigation areas. *Hydrol. Earth Syst. Sci.* **2005**, *9*, 535–547. [CrossRef]

28. Hoffman, R.O.; Edwards, D.E.; Wallin, G.; Burton, T. Remote sensing instrumentation and methods used for identifying center pivot sprinkler irrigation systems and estimating crop water use. *Proc. Int. Semin. Expo. Water Resour. Instrum.* **2013**, 312–317.

29. Loveland, T.R.; Reed, B.C.; Brown, J.F.; Ohlen, D.O.; Zhu, Z.; Yang, L.W.M.J.; Merchant, J.W. Development of a global land cover characteristics database and IGBP DISCover from 1 km AVHRR data. *Int. J. Remote Sens.* **2000**, *21*, 1303–1330. [CrossRef]

30. Deines, J.M.; Kendall, A.D.; Hyndman, D.W. Annual irrigation dynamics in the US Northern High Plains derived from Landsat satellite data. *Geophys. Res. Lett.* **2017**, *44*, 9350–9360. [CrossRef]

31. Peña-Arancibia, J.L.; McVicar, T.R.; Paydar, Z.; Li, L.; Guerschman, J.P.; Donohue, R.J.; Dutta, D.; Podger, G.M.; van Dijk, A.I.J.M.; Chiew, F.H.S. Dynamic identification of summer cropping irrigated areas in a large basin experiencing extreme climatic variability. *Remote Sens. Environ.* **2014**, *154*, 139–152. [CrossRef]

32. Ozdogan, M.; Gutman, G. A new methodology to map irrigated areas using multi-temporal MODIS and ancillary data: An application example in the continental US. *Remote Sens. Environ.* **2008**, *112*, 3520–3537. [CrossRef]

33. Nagaraj, D.; Proust, E.; Todeschini, A.; Rulli, M.C.; D'Odorico, P. A new dataset of global irrigation areas from 2001 to 2015. *Adv. Water Resour.* **2021**, *152*, 103910. [CrossRef]

34. Ambika, A.K.; Wardlow, B.; Mishra, V. Remotely sensed high resolution irrigated area mapping in India for 2000 to 2015. *Sci. Data* **2016**, *3*, 160118. [CrossRef] [PubMed]

35. Meier, J.; Zabel, F.; Mauser, W. A global approach to estimate irrigated areas—a comparison between different data and statistics. *Hydrol. Earth Syst. Sci.* **2018**, *22*, 1119–1133. [CrossRef]
36. Pervez, M.S.; Brown, J.F. Mapping irrigated lands at 250-m scale by merging MODIS data and national agricultural statistics. *Remote Sens.* **2010**, *2*, 2388–2412. [CrossRef]
37. Zhu, X.; Zhao, A.; Li, Y.; Liu, X. Agricultural irrigation requirements under future climate scenarios in China. *J. Arid. Land* **2015**, *7*, 224–237. [CrossRef]
38. Salmon, J.M.; Friedl, M.A.; Frolking, S.; Wisser, D.; Douglas, E.M. Global rain-fed, irrigated, and paddy croplands: A new high resolution map derived from remote sensing, crop inventories and climate data. *Int. J. Appl. Earth Obs. Geoinf.* **2015**, *38*, 321–334. [CrossRef]
39. Jin, N.; Tao, B.; Ren, W.; Feng, M.; Sun, R.; He, L.; Zhuang, W.; Yu, Q. Mapping irrigated and rainfed wheat areas using multi-temporal satellite data. *Remote Sens.* **2016**, *8*, 207. [CrossRef]
40. Chen, Y.; Lu, D.; Luo, L.; Pokhrel, Y.; Deb, K.; Huang, J.; Ran, Y. Detecting irrigation extent, frequency, and timing in a heterogeneous arid agricultural region using MODIS time series, Landsat imagery, and ancillary data. *Remote Sens. Environ.* **2018**, *204*, 197–211. [CrossRef]
41. Ferrant, S.; Caballero, Y.; Perrin, J.; Gascoin, S.; Dewandel, B.; Aulong, S.; Dazin, F.; Ahmed, S.; Maréchal, J.C. Projected impacts of climate change on farmers' extraction of groundwater from crystalline aquifers in South India. *Sci. Rep.* **2014**, *4*, 1377–1406. [CrossRef] [PubMed]
42. Ferrant, S.; Selles, A.; Le Page, M.; Herrault, P.-A.; Pelletier, C.; Al-Bitar, A.; Mermoz, S.; Gascoin, S.; Bouvet, A.; Saqalli, M.; et al. Detection of irrigated crops from sentinel-1 and sentinel-2 data to estimate seasonal groundwater use in South India. *Remote Sens.* **2017**, *9*, 1119. [CrossRef]
43. Ferrant, S.; Selles, A.; Le Page, M.; AlBitar, A.; Mermoz, S.; Gascoin, S.; Bouvet, A.; Ahmed, S.; Kerr, Y. Sentinel-1&2 for near real time cropping pattern monitoring in drought prone areas. application to irrigation water needs in telangana, south-india. *Int. Arch. Photogramm. Remote Sens. Spat. Inf. Sci.* **2019**, *42*, 285–292. [CrossRef]
44. Demarez, V.; Helen, F.; Marais-Sicre, C.; Baup, F. In-season mapping of irrigated crops using landsat 8 and sentinel-1 time series. *Remote Sens.* **2019**, *11*, 118. [CrossRef]
45. Pageot, Y.; Baup, F.; Inglada, J.; Baghdadi, N.; Demarez, V. Detection of irrigated and rainfed crops in temperate areas using sentinel-1 and sentinel-2 time series. *Remote Sens.* **2020**, *12*, 3044. [CrossRef]
46. Deines, J.M.; Kendall, A.D.; Crowley, M.A.; Rapp, J.; Cardille, J.A.; Hyndman, D.W. Mapping three decades of annual irrigation across the US high plains aquifer using landsat and Google Earth Engine. *Remote Sens. Environ.* **2019**, *233*, 111400. [CrossRef]
47. Xu, X.; Chen, F.; Barlage, M.; Gochis, D.; Miao, S.; Shen, S. Lessons learned from modeling irrigation from field to regional scales. *J. Adv. Modeling Earth Syst.* **2019**, *11*, 2428–2448. [CrossRef]
48. Zohaib, M.; Kim, H.; Choi, M. Detecting global irrigated areas by using satellite and reanalysis products. *Sci. Total. Environ.* **2019**, *677*, 679–691. [CrossRef] [PubMed]
49. McAllister, A.; Whitfield, D.; Abuzar, M. Mapping irrigated farmlands using vegetation and thermal thresholds derived from landsat and ASTER data in an irrigation district of Australia. *Photogramm. Eng. Remote Sens.* **2015**, *81*, 229–238. [CrossRef]
50. Pun, M.; Mutiibwa, D.; Li, R. Land use classification: A surface energy balance and vegetation index application to map and monitor irrigated lands. *Remote Sens.* **2017**, *9*, 1256. [CrossRef]
51. Duchemin, B.; Hadria, R.; Erraki, S.; Boulet, G.; Maisongrande, P.; Chehbouni, A.; Escadafal, R.; Ezzahar, J.; Hoedjes, J.C.B.; Kharrou, M.H.; et al. Monitoring wheat phenology and irrigation in Central Morocco: On the use of relationships between evapotranspiration, crops coefficients, leaf area index and remotely-sensed vegetation indices. *Agric. Water Manag.* **2006**, *79*, 1–27. [CrossRef]
52. Consoli, S.; Cirelli, G.L.; Toscano, A. Monitoring crop coefficient of orange orchards using energy balance and the remote sensed NDVI. In *Remote Sensing for Agriculture, Ecosystems, and Hydrology VIII*; Owe, M., D'Urso, G., Neale, C.M.U., Gouweleeuw, B.T., Eds.; SPIE: Stockholm, Sweden, 2006; Volume 6359, pp. 179–189. [CrossRef]
53. de Oliveira, R.M.; da Cunha, F.F.; da Silva, G.H.; Andrade, L.M.; de Morais, C.V.; Ferreira, P.M.O.; Raimundi, F.P.G.; Freitas, A.R.; de Souza, C.M.; de Oliveira, R.A. Evapotranspiration and crop coefficients of Italian zucchini cultivated with recycled paper as mulch. *PLoS ONE* **2020**, *15*, 1–16. [CrossRef]
54. French, A.N.; Hunsaker, D.J.; Sanchez, C.A.; Saber, M.; Gonzalez, J.R.; Anderson, R. Satellite-based NDVI crop coefficients and evapotranspiration with eddy covariance validation for multiple durum wheat fields in the US Southwest. *Agric. Water Manag.* **2020**, *239*, 106266. [CrossRef]
55. Guerschman, J.P.; Van Dijk, A.I.J.M.; Mattersdorf, G.; Beringer, J.; Hutley, L.B.; Leuning, R.; Pipunic, R.C.; Sherman, B.S. Scaling of potential evapotranspiration with MODIS data reproduces flux observations and catchment water balance observations across Australia. *J. Hydr.* **2009**, *369*, 107–119. [CrossRef]
56. Hunsaker, D.J.; Fitzgerald, G.J.; French, A.N.; Clarke, T.R.; Ottman, M.J.; Pinter, P.J. Wheat irrigation management using multispectral crop coefficients: I. Crop evapotranspiration prediction. *Trans. ASABE* **2007**, *50*, 2017–2033. [CrossRef]
57. Kamble, B.; Kilic, A.; Hubbard, K.; French, A.; Hunsaker, D.; Sanchez, C.A.; Saber, M.; Gonzalez, J.R.; Anderson, R.; Farg, E.; et al. Estimation of evapotranspiration ETc and crop coefficient Kc of wheat, in south nile delta of egypt using integrated FAO-56 approach and remote sensing data. *Remote Sens.* **2012**, *239*, 83–89. [CrossRef]

58. Kamble, B.; Kilic, A.; Hubbard, K. Estimating crop coefficients using remote sensing-based vegetation index. *Remote Sens.* **2013**, *5*, 1588–1602. [CrossRef]

59. Mutiibwa, D.; Irmak, S. AVHRR-NDVI-based crop coefficients for analyzing long-term trends in evapotranspiration in relation to changing climate in the U.S. High Plains. *Water Resour. Res.* **2013**, *49*, 231–244. [CrossRef]

60. Allen, R.G.; Pereira, L.; Raes, D.; Smith, M. *FAO Irrigation and Drainage Paper No. 56*; Food and Agriculture Organization of the United Nations: Rome, Italy, 1998; Volume 56, pp. 26–40.

61. Allen, R.G.; Pereira, L.; Smith, M.; Raes, D.; Wright, J.L. FAO-56 dual crop coefficient method for estimating evaporation from soil and application extensions. *J. Irrig. Drain. Eng.* **2005**, *131*, 2–13. [CrossRef]

62. Hunink, J.E.; Eekhout, J.P.C.; de Vente, J.; Contreras, S.; Droogers, P.; Baille, A. Hydrological modelling using satellite-based crop coefficients: A comparison of methods at the basin scale. *Remote Sens.* **2017**, *9*, 174. [CrossRef]

63. Hunsaker, D.J.; Pinter, P.J.; Barnes, E.M.; Kimball, B.A. Estimating cotton evapotranspiration crop coefficients with a multispectral vegetation index. *Irrig. Sci.* **2003**, *22*, 95–104. [CrossRef]

64. Zhang, Y.; Han, W.; Niu, X.; Li, G. Maize crop coefficient estimated from UAV-Measured multispectral vegetation indices. *Sensors* **2019**, *19*, 5250. [CrossRef]

65. Saadi, S.; Todorovic, M.; Tanasijevic, L.; Pereira, L.S.; Pizzigalli, C.; Lionello, P. Climate change and Mediterranean agriculture: Impacts on winter wheat and tomato crop evapotranspiration, irrigation requirements and yield. *Agric. Water Manag. Agric. Water Manag. Priorities Chall.* **2015**, *147*, 103–115. [CrossRef]

66. Droogers, P.; Immerzeel, W.W.; Lorite, I.J. Estimating actual irrigation application by remotely sensed evapotranspiration observations. *Agric. Water Manag.* **2010**, *97*, 1351–1359. [CrossRef]

67. Romaguera, M.; Hoekstra, A.Y.; Su, Z.; Krol, M.S.; Salama, M.S. Potential of using remote sensing techniques for global assessment of water footprint of crops. *Remote Sens.* **2010**, *2*, 1177–1196. [CrossRef]

68. Van Dijk, A.I.J.M.; Schellekens, J.; Yebra, M.; Beck, H.E.; Renzullo, L.J.; Weerts, A.; Donchyts, G. Global 5 km resolution estimates of secondary evaporation including irrigation through satellite data assimilation. *Hydrol. Earth Syst. Sci.* **2018**, *22*, 4959–4980. [CrossRef]

69. Van Eekelen, M.W.; Bastiaanssen, W.G.; Jarmain, C.; Jackson, B.; Ferreira, F.; Van der Zaag, P.; Okello, A.S.; Bosch, J.; Dye, P.; Boastidas-Obando, E.; et al. A novel approach to estimate direct and indirect water withdrawals from satellite measurements: A case study from the Incomati basin. *Agric. Ecosyst. Environ.* **2015**, *200*, 126–142. [CrossRef]

70. Bastiaanssen, W.G.M.; Menenti, M.; Feddes, R.A.; Holtslag, A.A.M. A remote sensing surface energy balance algorithm for land (SEBAL). 1. Formulation. *J. Hydrol.* **1998**, *212*, 198–212. [CrossRef]

71. Bastiaanssen, W.G.M.; Pelgrum, H.; Wang, J.; Ma, Y.; Moreno, J.F.; Roerink, G.J.; van der Wal, T. A remote sensing surface energy balance algorithm for land (SEBAL): 2. Validation. *J. Hydrol.* **1998**, *212*, 213–229. [CrossRef]

72. Hain, C.R.; Crow, W.T.; Anderson, M.C.; Yilmaz, M.T. Diagnosing neglected soil moisture source–sink processes via a thermal infrared–based two-source energy balance model. *J. Hydrometeorol.* **2015**, *16*, 1070–1086. [CrossRef]

73. Peña-Arancibia, J.L.; Mainuddin, M.; Kirby, J.M.; Chiew, F.H.; McVicar, T.R.; Vaze, J. Assessing irrigated agriculture's surface water and groundwater consumption by combining satellite remote sensing and hydrologic modelling. *Sci. Total. Environ.* **2016**, *542*, 372–382. [CrossRef] [PubMed]

74. Olivera-Guerra, L.; Merlin, O.; Er-Raki, S. Irrigation retrieval from Landsat optical/thermal data integrated into a crop water balance model: A case study over winter wheat fields in a semi-arid region. *Remote Sens. Environ.* **2020**, *239*, 111627. [CrossRef]

75. Vogels, M.F.A.; de Jong, S.M.; Sterk, G.; Wanders, N.; Bierkens, M.F.P.; Addink, E.A. An object-based image analysis approach to assess irrigation-water consumption from MODIS products in Ethiopia. *Int. J. Appl. Earth Obs. Geoinf.* **2020**, *88*, 102067. [CrossRef]

76. Bastiaanssen, W.G.M.; Karimi, P.; Rebelo, L.M.; Duan, Z.; Senay, G.; Muthuwatte, L.; Smakhtin, V. Earth observation based assessment of the water production and water consumption of Nile basin agro-ecosystems. *Remote Sens.* **2014**, *6*, 10306–10334. [CrossRef]

77. Maselli, F.; Battista, P.; Chiesi, M.; Rapi, B.; Angeli, L.; Fibbi, L.; Magno, R.; Gozzini, B. Use of sentinel-2 MSI data to monitor crop irrigation in Mediterranean areas. *Int. J. Appl. Earth Obs. Geoinf.* **2020**, *93*, 102216. [CrossRef]

78. Aragon, B.; Houborg, R.; Tu, K.; Fisher, J.B.; McCabe, M. CubeSats enable high spatiotemporal retrievals of crop-water use for precision agriculture. *Remote Sens.* **2018**, *10*, 1867. [CrossRef]

79. Kumar, S.V.; Peters-Lidard, C.D.; Santanello, J.A.; Reichle, R.H.; Draper, C.S.; Koster, R.D. Evaluating the utility of satellite soil moisture retrievals over irrigated areas and the ability of land data assimilation methods to correct for unmodelled processes. *Hydrol. Earth Syst. Sci.* **2015**, *19*, 4463–4478. [CrossRef]

80. Escorihuela, M.J.; Quintana-Segui, P. Comparison of remote sensing and simulated soil moisture data sets in Mediterranean landscapes. *Remote Sens. Environ.* **2016**, *180*, 99–114. [CrossRef]

81. Malbéteau, Y.; Merlin, O.; Balsamo, G.; Er-Raki, S.; Khabba, S.; Walker, J.P.; Jarlan, L. Towards a surface soil moisture product at high spatio-temporal resolution: Temporally-interpolated spatially-disaggregated SMOS data. *J. Hydrometeorol.* **2018**, *19*, 183–200. [CrossRef]

82. Singh, D.; Gupta, P.K.; Pradhan, R.; Dubey, A.K.; Singh, R.P. Discerning shifting irrigation practices from passive microwave radiometry over Punjab and Haryana. *J. Water Clim. Chang.* **2017**, *8*, 303–319. [CrossRef]

83. Lawston, P.M.; Santanello, J.A.; Kumar, S.V. Irrigation signals detected from SMAP soil moisture retrievals. *Geophys. Res. Lett.* **2017**, *44*, 11860–11867. [CrossRef]

84. Fontanet, M.; Fernàndez-Garcia, D.; Ferrer, F. The value of satellite remote sensing soil moisture data and the DISPATCH algorithm in irrigation fields. *Hydrol. Earth Syst. Sci.* **2018**, *22*, 5889–5900. [CrossRef]

85. Merlin, O.; Chehbouni, G.; Walker, J.P.; Panciera, R.; Kerr, Y.H. A simple method for downscaling passive microwave based soil moisture. *IEEE Geosci. Remote. Sens. Lett.* **2008**, *46*, 786–796. [CrossRef]

86. Dari, J.; Quintana-Seguí, P.; Escorihuela, M.J.; Stefan, V.; Brocca, L.; Morbidelli, R. Detecting and mapping irrigated areas in a Mediterranean environment by using remote sensing soil moisture and a land surface model. *J. Hydrol.* **2021**, *596*, 126129. [CrossRef]

87. El Hajj, M.; Baghdadi, N.; Belaud, G.; Zribi, M.; Cheviron, B.; Courault, D.; Charron, F. Irrigated grassland monitoring using a time series of TerraSAR-X and COSMO-SkyMed X-band SAR data. *Remote Sens.* **2014**, *6*, 10002–10032. [CrossRef]

88. El Hajj, M.; Baghdadi, N.; Zribi, M.; Bazzi, H. Synergetic use of Sentinel1 and Sentinel2 images for operational soil moisture mapping at high spatial resolution over agricultural areas. *Remote Sens.* **2017**, *9*, 1292. [CrossRef]

89. Santi, E.; Dabboor, M.; Pettinato, S.; Paloscia, S. Combining machine learning and compact polarimetry for estimating soil moisture from C-Band SAR data. *Remote Sens.* **2019**, *11*, 2451. [CrossRef]

90. Gao, Q.; Zribi, M.; Escorihuela, M.; Baghdadi, N. Synergetic use of Sentinel-1 and Sentinel-2 data for soil moisture mapping at 100 m resolution. *Sensors* **2017**, *17*, 1966. [CrossRef]

91. Bauer-Marschallinger, B.; Freeman, V.; Cao, S.; Paulik, C.; Schaufler, S.; Stachl, T.; Modanesi, S.; Massari, C.; Ciabatta, L.; Brocca, L. Toward global soil moisture monitoring with sentinel-1: Harnessing assets and overcoming obstacles. *IEEE Trans. Geosci. Remote Sens.* **2018**, *57*, 520–539. [CrossRef]

92. Bousbih, S.; Zribi, M.; El Hajj, M.; Baghdadi, N.; Lili-Chabaane, Z.; Gao, Q.; Fanise, P. Soil moisture and irrigation mapping in a semi-arid region based on the synergic use of Sentinel-1 and Sentinel-2 data. *Remote Sens.* **2018**, *10*, 1953. [CrossRef]

93. Gao, Q.; Zribi, M.; Escorihuela, M.; Baghdadi, N.; Segui, P. Irrigation mapping using Sentinel-1 time series at field scale. *Remote Sens.* **2018**, *10*, 1495. [CrossRef]

94. Bazzi, H.; Baghdadi, N.; Ienco, D.; El Hajj, M.; Zribi, M.; Belhouchette, H.; Escorihuela, M.J.; Demarez, V. Mapping irrigated areas using sentinel-1 time series in Catalonia, Spain. *Remote Sens.* **2019**, *11*, 1836. [CrossRef]

95. Bazzi, H.; Baghdadi, N.; Fayad, I.; Zribi, M.; Belhouchette, H.; Demarez, V. Near real-time irrigation detection at plot scale using sentinel-1 data. *Remote Sens.* **2020**, *12*, 1456. [CrossRef]

96. Dari, J.; Brocca, L.; Quintana-Seguí, P.; Casadei, S.; Escorihuela, M.J.; Stefan, V.; Morbidelli, R. Double-scale analysis on the detectability of irrigation signals from remote sensing soil moisture over an area with complex topography in central Italy. *Adv. Water Resour.* **2021**. under review.

97. Brocca, L.; Tarpanelli, A.; Filippucci, P.; Dorigo, W.; Zaussinger, F.; Gruber, A.; Fernández-Prieto, D. How much water is used for irrigation? A new approach exploiting coarse resolution satellite soil moisture products. *Int. J. Appl. Earth Obs. Geoinf.* **2018**, *73C*, 752–766. [CrossRef]

98. Jalilvand, E.; Tajrishy, M.; Hashemi, S.A.G.; Brocca, L. Quantification of irrigation water using remote sensing of soil moisture in a semi-arid region. *Remote. Sens. Environ.* **2019**, *231*, 111226. [CrossRef]

99. Zhang, X.; Qiu, J.; Leng, G.; Yang, Y.; Gao, Q.; Fan, Y.; Luo, J. The potential utility of satellite soil moisture retrievals for detecting irrigation patterns in China. *Water* **2018**, *10*, 1505. [CrossRef]

100. Zaussinger, F.; Dorigo, W.; Gruber, A.; Tarpanelli, A.; Filippucci, P.; Brocca, L. Estimating irrigation water use over the contiguous United States by combining satellite and reanalysis soil moisture data. *Hydrol. Earth Syst. Sci.* **2019**, *23*, 897–923. [CrossRef]

101. Zohaib, M.; Choi, M. Satellite-based global-scale irrigation water use and its contemporary trends. *Sci. Total. Environ.* **2020**, *714*, 136719. [CrossRef] [PubMed]

102. Dari, J.; Brocca, L.; Quintana-Seguí, P.; Escorihuela, M.J.; Stefan, V.; Morbidelli, R. Exploiting high-resolution remote sensing soil moisture to estimate irrigation water amounts over a mediterranean region. *Remote Sens.* **2020**, *12*, 2593. [CrossRef]

103. Zappa, L.; Schlaffer, S.; Bauer-Marschallinger, B.; Nendel, C.; Zimmerman, B.; Dorigo, W. Detection and quantification of irrigation water amounts at 500 m using sentinel-1 surface soil moisture. *Remote Sens.* **2021**, *13*, 1727. [CrossRef]

104. Tapley, B.D.; Bettadpur, S.; Ries, J.C.; Thompson, P.F.; Watkins, M.M. GRACE measurements of mass variability in the Earth system. *Science* **2004**, *305*, 503–505. [CrossRef]

105. Landerer, F.W.; Flechtner, F.M.; Save, H.; Webb, F.H.; Bandikova, T.; Bertiger, W.I.; Bettadpur, S.V.; Byun, S.H.; Dahle, C.; Dobslaw, H.; et al. Extending the global mass change data record: GRACE Follow-On instrument and science data performance. *Geophys. Res. Let.* **2020**, *47*, e2020GL088306. [CrossRef]

106. Rodell, M.; Famiglietti, J.S.; Wiese, D.N.; Reager, J.T.; Beaudoing, H.K.; Landerer, F.W.; Lo, M.H. Emerging trends in global freshwater availability. *Nature* **2018**, *557*, 651–659. [CrossRef]

107. Save, H.; Bettadpur, S.; Tapley, B.D. High-resolution CSR GRACE RL05 mascons. *J. Geophys. Res. Solid Earth* **2016**, *121*, 7547–7569. [CrossRef]

108. Kueppers, L.M.; Snyder, M.A.; Sloan, L.C. Irrigation cooling effect: Regional climate forcing by land-use change. *Geophys. Res. Let.* **2007**, *34*, L03703. [CrossRef]

109. Lobell, D.; Bala, G.; Mirin, A.; Phillips, T.; Maxwell, R.; Rotman, D. Regional differences in the influence of irrigation on climate. *J. Clim.* **2009**, *22*, 2248–2255. [CrossRef]

110. Wada, Y.; Bierkens, M.F.P.; De Roo, A.; Dirmeyer, P.A.; Famiglietti, J.S.; Hanasaki, N.; Konar, M.; Liu, J.; Müller Schmied, H.; Oki, T.; et al. Human–water interface in hydrological modelling: Current status and future directions. *Hydrol. Earth Syst. Sci.* **2017**, *21*, 4169–4193. [CrossRef]

111. Ozdogan, M.; Rodell, M.; Beaudoing, H.K.; Toll, D. Simulating the effects of irrigation over the US in a land surface model based on satellite derived agricultural data. *J. Hydrometeor.* **2010**, *11*, 171–184. [CrossRef]

112. Chen, F.; Mitchell, K.; Schaake, J.; Xue, Y.; Pan, H.L.; Koren, V.; Duan, Q.Y.; Ek, M.; Betts, A. Modeling of land surface evaporation by four schemes and comparison with fife observations. *J. Geophys. Res.-Atmos.* **1996**, *101*, 7251–7268. [CrossRef]

113. Evans, J.P.; Zaitchik, B.F. Modeling the large-scale water balance impact of different irrigation systems. *Water Resour. Res.* **2008**, *44*, W08448. [CrossRef]

114. Lawston, P.M.; Santanello, J.A.; Zaitchik, B.F.; Rodell, M. Impact of irrigation methods on land surface model spinup and initialization of WRF forecasts. *J. Hydrometeorol.* **2015**, *16*, 1135–1154. [CrossRef]

115. Pokhrel, Y.; Hanasaki, N.; Koirala, S.; Cho, J.; Yeh, P.J.F.; Kim, H.; Kanae, S.; Oki, T. Incorporating anthropogenic water regulation modules into a land surface model. *J. Hydrometeorol.* **2012**, *13*, 255–269. [CrossRef]

116. De Rosnay, P.; Polcher, J.; Laval, K.; Sabre, M. Integrated parameterization of irrigation in the land surface model ORCHIDEE. Validation over Indian Peninsula. *Geophys. Res. Lett.* **2003**, *30*. [CrossRef]

117. Girotto, M.; De Lannoy, G.J.M.; Reichle, R.H.; Rodell, M.; Draper, C.; Bhanja, S.N.; Mukherjee, A. Benefits and pitfalls of GRACE data assimilation: A case study of terrestrial water storage depletion in India. *Geophys. Res. Lett.* **2017**, *44*, 4107–4115. [CrossRef]

118. Nie, W.; Zaitchik, B.F.; Rodell, M.; Kumar, S.V.; Anderson, M.C.; Hain, C. Groundwater withdrawals under drought: Reconciling GRACE and land surface models in the United States High Plains Aquifer. *Water Resour. Res.* **2018**, *54*, 5282–5299. [CrossRef]

119. Nie, W.; Zaitchik, B.F.; Rodell, M.; Kumar, S.V.; Arsenault, K.R.; Li, B.; Getirana, A. Assimilating GRACE into a land surface model in the presence of an irrigation-induced groundwater trend. *Water Resour. Res.* **2019**, *55*, 11274–11294. [CrossRef]

120. Cook, B.I.; Shukla, S.P.; Puma, M.J.; Nazarenko, L.S. Irrigation as an historical climate forcing. *Clim. Dyn.* **2015**, *44*, 1715–1730. [CrossRef]

121. Lee, E.; Sacks, W.J.; Chase, T.N.; Foley, J.A. Simulated impacts of irrigation on the atmospheric circulation over Asia. *J. Geophys. Res.* **2011**, *116*, D08114. [CrossRef]

122. Boucher, O.; Myhre, G.; Myhre, A. Direct human influence of irrigation on atmospheric water vapour and climate. *Clim. Dyn.* **2004**, *22*, 597–603. [CrossRef]

123. Badger, A.M.; Dirmeyer, P.A. Climate response to Amazon forest replacement by heterogeneous crop cover. *Hydrol. Earth Syst. Sci.* **2015**, *19*, 4547–4557. [CrossRef]

124. Jiang, L.-M.; Lak, B.; Eijsvogels, L.M.; Wesselink, P.; van der Sluis, L.W.M. Comparison of the cleaning efficacy of different final irrigation techniques. *J. Endod.* **2012**, *38*, 838–841. [CrossRef]

125. Tang, J.-L.; Zhang, B.; Zepp, H. Estimation of irrigation flow by hydrograph analysis in a complex agricultural catchment in subtropical China. *Hydrol. Process.* **2007**, *21*, 1280–1288. [CrossRef]

126. Haddeland, I.; Lettenmaier, D.P.; Skaugen, T. Effects of irrigation on the water and energy balances of the Colorado and Mekong river basins. *J. Hydrol.* **2006**, *324*, 210–223. [CrossRef]

127. Yilmaz, M.T.; Anderson, M.C.; Zaitchik, B.; Hain, C.R.; Crow, W.T.; Ozdogan, M.; Chun, J.A.; Evans, J. Comparison of prognostic and diagnostic surface flux modeling approaches over the Nile River basin. *Water Resour. Res.* **2014**, *50*, 386–408. [CrossRef]

128. Li, J.; Mahalov, A.; Hyde, P. Impacts of agricultural irrigation on ozone concentrations in the Central Valley of California and in the contiguous United States based on WRF-Chem simulations. *Agric. For. Meteorol.* **2016**, *221*, 34–49. [CrossRef]

129. Mahalov, A.; Li, J.; Hyde, P. Regional impacts of irrigation in Mexico and southwestern U.S. on hydrometeorological fields in the North American Monsoon region. *J. Hydrometeorol.* **2016**, *17*, 2981–2995. [CrossRef]

130. Scanlon, B.R.; Zhang, Z.; Save, H.; Sun, A.Y.; Schmied, H.M.; Van Beek, L.P.; Wiese, D.N.; Wada, Y.; Long, D.; Reedy, R.C.; et al. Global models underestimate large decadal declining and rising water storage trends relative to GRACE satellite data. *Proc. Natl. Acad. Sci. USA* **2018**, *115*, E1080–E1089. [CrossRef]

131. Arnold, J.G.; Moriasi, D.N.; Gassman, P.W.; Abbaspour, K.C.; White, M.J.; Srinivasan, R.; Santhi, C.; Harmel, R.D.; van Griensven, A.; Liew, M.W.V.; et al. SWAT: Model use, calibration, and validation. *Trans. ASABE* **2012**, *55*, 1491–1508. [CrossRef]

132. Alcamo, J.; Döll, P.; Henrichs, T.; Kaspar, F.; Lehner, B.; Rösch, T.; Siebert, S. Development and testing of the WaterGAP 2 global model of water use and availability. *Hydrolog. Sci. J.* **2003**, *48*, 317–337. [CrossRef]

133. Wisser, D.; Frolking, S.; Douglas, E.M.; Fekete, B.M.; Schumann, A.H.; Vörösmarty, C.J. The significance of local water resources captured in small reservoirs for crop production–A global-scale analysis. *J. Hydrol.* **2010**, *384*, 264–275. [CrossRef]

134. Sanz, D.; Calera, A.; Castaño, S.; Gómez-Alday, J.J. Knowledge, participation and transparency in groundwater management. *Water Policy* **2016**, *18*, 111–125. [CrossRef]

135. WUEMoCA. Available online: https://wuemoca.geo.uni-halle.de/app/ (accessed on 29 July 2021).

136. FAO. *WaPOR Database Methodology*; Version 2 release; FAO: Rome, Italy, 2020. [CrossRef]

137. Foster, T.; Mieno, T.; Brozovic, N. Satellite-based monitoring of irrigation water use: Assessing measurement errors and their implications for agricultural water management policy. *Water Resour. Res.* **2020**, *56*. [CrossRef]

138. García-Mollá, M.; Sanchis-Ibor, C.; Avellà-Reus, L.; Albiac, J.; Isidoro, D.; Lecina, S. Spain. In *Irrigation in the Mediterranean*; Springer: Berlin/Heidelberg, Germany, 2019; pp. 89–121. [CrossRef]

139. Linés, C.; Iglesias, A.; Garrote, L.; Sotés, V.; Werner, M. Do users benefit from additional information in support of operational drought management decisions in the Ebro basin? *Hydrol. Earth Syst. Sci.* **2018**, *22*, 5901–5917. [CrossRef]

140. Molle, F.; Sanchis-Ibor, C. Irrigation policies in the mediterranean: Trends and challenges. In *Irrigation in the Mediterranean: Technologies, Institutions and Policies, Global Issues in Water Policy*; Molle, F., Sanchis-Ibor, C., Avellà-Reus, L., Eds.; Springer International Publishing: Cham, Switzerland, 2019; pp. 279–313. [CrossRef]

141. Lagouarde, J.-P.; Bhattacharya, B.; Crébassol, P.; Gamet, P.; Adlakha, D.; Murthy, C.; Singh, S.; Mishra, M.; Nigam, R.; Raju, P.; et al. Indo-french high-resolution thermal infrared space mission for earth natural resources assessment and monitoring-concept and definition of TRISHNA. In Proceedings of the ISPRS-GEOGLAM-ISRS Joint International Workshop on "Earth Observations for Agricultural Monitoring", New Delhi, India, 18–20 February 2019; p. 403. [CrossRef]

142. Koetz, B.; Bastiaanssen, W.; Berger, M.; Defourney, P.; Del Bello, U.; Drusch, M.; Drinkwater, M.; Duca, R.; Fernandez, V.; Ghent, D.; et al. High spatio-temporal resolution land surface temperature mission—a copernicus candidate mission in support of agricultural monitoring. In Proceedings of the IGARSS 2018—2018 IEEE International Geoscience and Remote Sensing Symposium, Valencia, Spain, 5 November 2018; pp. 8160–8162. [CrossRef]

143. Senay, G.B.; Friedrichs, M.; Singh, R.K.; Velpuri, N.M. Evaluating Landsat 8 evapotranspiration for water use mapping in the Colorado River Basin. *Remote Sens. Environ.* **2016**, *185*, 171–185. [CrossRef]

144. Guzinski, R.; Nieto, H.; Sandholt, I.; Karamitilios, G. Modelling high-resolution actual evapotranspiration through sentinel-2 and sentinel-3 data fusion. *Remote Sens.* **2020**, *12*, 1433. [CrossRef]

145. Velpuri, N.M.; Senay, G.B.; Schauer, M.; Garcia, C.A.; Singh, R.K.; Friedrichs, M.; Kagone, S.; Haynes, J.; Conlon, T. Evaluation of hydrologic impact of an irrigation curtailment program using Landsat satellite data. *Hydrol. Process.* **2020**, *34*, 1697–1713. [CrossRef]

146. Ragettli, S.; Herberz, T.; Siegfried, T. An unsupervised classification algorithm for multi-temporal irrigated area mapping in central Asia. *Remote Sens.* **2018**, *10*, 1823. [CrossRef]

147. Wang, S.; Azzari, G.; Lobell, D.B. Crop type mapping without field-level labels: Random forest transfer and unsupervised clustering techniques. *Remote Sens. Environ.* **2019**, *222*, 303–317. [CrossRef]

148. Chou, C.; Ryu, D.; Lo, M.H.; Wey, H.W.; Malano, H.M. Irrigation-induced land–atmosphere feedbacks and their impacts on Indian summer monsoon. *J. Clim.* **2018**, *31*, 8785–8801. [CrossRef]

149. Famiglietti, J.S. The global groundwater crisis. *Nat. Clim. Chang.* **2014**, *4*, 945–948. [CrossRef]

150. Modanesi, S.; Massari, C.; Gruber, A.; Lievens, H.; Tarpanelli, A.; Morbidelli, R.; De Lannoy, G.J.M. Optimizing a backscatter forward operator using Sentinel-1 data over irrigated land. *Hydrol. Earth Syst. Sci. Discuss.* **2021**, 1–39. [CrossRef]

151. Chew, C.C.; Small, E.E. Soil moisture sensing using spaceborne GNSS reflections: Comparison of CYGNSS reflectivity to SMAP soil moisture. *Geophys. Res. Lett.* **2018**, *45*, 4049–4057. [CrossRef]

152. Kim, H.; Lakshmi, V. Use of cyclone global navigation satellite system (CyGNSS) observations for estimation of soil moisture. *Geophys. Res. Let.* **2018**, *45*, 8272–8282. [CrossRef]

153. ROSE-L. 2018, Copernicus L-band SAR Mission Requirements Document, ESA, ESA-EOPSM-CLIS-MRD-3371, NISAR, 2018. NASA-ISRO SAR (NISAR) Mission Science Users' Handbook. NASA Jet Propulsion Laboratory. 261p. 2018. Available online: https://nisar.jpl.nasa.gov/system/documents/files/26_NISAR_FINAL_9-6-19.pdf (accessed on 13 October 2021).